BBA - General Subjects 1865 (2021) 129854

Contents lists available at ScienceDirect

BBA - General Subjects

journal homepage: www.elsevier.com/locate/bbagen

The mitochondrial aspartate/glutamate carrier (AGC or Aralar1) isoforms in *D. melanogaster*: biochemical characterization, gene structure, and evolutionary analysis

Paola Lunetti [a,1], René Massimiliano Marsano [b,1], Rosita Curcio [c,1], Vincenza Dolce [c,*], Giuseppe Fiermonte [d], Anna Rita Cappello [c], Federica Marra [c], Roberta Moschetti [b], Yuan Li [c,e], Donatella Aiello [f], Araceli del Arco Martínez [g], Graziantonio Lauria [c], Francesco De Leonardis [d], Alessandra Ferramosca [a], Vincenzo Zara [a,*], Loredana Capobianco [a,*]

[a] *Department of Biological and Environmental Sciences and Technologies, University of Salento, 73100 Lecce, Italy*
[b] *Department of Biology, University of Bari, 70125 Bari, Italy*
[c] *Department of Pharmacy, Health, and Nutritional Sciences, University of Calabria, 87036, Arcavacata di Rende, Cosenza, Italy*
[d] *Department of Biosciences, Biotechnologies and Biopharmaceutics, University of Bari, 70125 Bari, Italy*
[e] *Faculty of Biological Engineering, Sichuan University of Science and Engineering, Yibin, China*
[f] *Department of Chemistry, University of Calabria, 87036, Arcavacata di Rende, Cosenza, Italy*
[g] *Facultad de Ciencias del Medio Ambiente, Universidad de Castilla La Mancha, Toledo, Spain*

ARTICLE INFO

Keywords:
Drosophila melanogaster
CG2139
Aspartate/glutamate carrier (AGC)
Aralar
Citrin
Phylogenetic footprint

ABSTRACT

Background: In man two mitochondrial aspartate/glutamate carrier (AGC) isoforms, known as aralar and citrin, are required to accomplish several metabolic pathways. In order to fill the existing gap of knowledge in *Drosophila melanogaster*, we have studied *aralar1* gene, orthologue of human AGC-encoding genes in this organism.

Methods: The blastp algorithm and the "reciprocal best hit" approach have been used to identify the human orthologue of AGCs in Drosophilidae and non-Drosophilidae. Aralar1 proteins have been overexpressed in *Escherichia coli* and functionally reconstituted into liposomes for transport assays.

Results: The transcriptional organization of *aralar1* comprises six isoforms, three constitutively expressed (*aralar1-RA, RD and RF*), and the remaining three distributed during the development or in different tissues (*aralar1-RB, RC and RE*). Aralar1-PA and Aralar1-PE, representative of all isoforms, have been biochemically characterized. Recombinant Aralar1-PA and Aralar1-PE proteins share similar efficiency to exchange glutamate against aspartate, and same substrate affinities than the human isoforms. Interestingly, although Aralar1-PA and Aralar1-PE diverge only in their EF-hand 8, they greatly differ in their specific activities and substrate specificity.

Conclusions: The tight regulation of aralar1 transcripts expression and the high request of aspartate and glutamate during early embryogenesis suggest a crucial role of Aralar1 in this Drosophila developmental stage. Furthermore, biochemical characterization and calcium sensitivity have identified Aralar1-PA and Aralar1-PE as the human aralar and citrin counterparts, respectively.

General significance: The functional characterization of the fruit fly mitochondrial AGC transporter represents a crucial step toward a complete understanding of the metabolic events acting during early embryogenesis.

Abbreviations: AGC, aspartate/glutamate carrier; MAS, malate-aspartate shuttle; MCF, mitochondrial carrier family; NRG, nuclear respiratory gene; SDS-PAGE, polyacrylamide gel electrophoresis in the presence of sodium dodecyl sulfate; TSS, transcriptional start site.

* Corresponding authors.
E-mail addresses: vincenza.dolce@unical.it (V. Dolce), vincenzo.zara@unisalento.it (V. Zara), loredana.capobianco@unisalento.it (L. Capobianco).

[1] These authors contributed equally to this work.

https://doi.org/10.1016/j.bbagen.2021.129854
Received 18 July 2020; Received in revised form 18 January 2021; Accepted 19 January 2021
Available online 23 January 2021

1. Introduction

The mitochondrial carrier family (MCF) represents one of the largest families of transporters widespread across all species. MCF members share a common structural organization, consisting of three tandemly repeated sequences of approximately 100 amino acids in length, and mediate the transport of metabolites across the inner mitochondrial membrane [1–3]. The aspartate/glutamate carrier (AGC) catalyzes an electrogenic exchange of cytosolic glutamate plus a proton for mitochondrial aspartate [4], and it is one of the most important family member, since it is a key component of the malate-aspartate shuttle (MAS), which transfers the reducing equivalents of NADH from cytosol to mitochondria in order to regenerate NAD^+ necessary for glycolysis. Furthermore, AGC plays an essential role in many other metabolic processes including the synthesis of urea and nitrogen-containing metabolites [5], gluconeogenesis from lactate [5], calcium-mediated regulation of mitochondrial respiration [4,6–9], insulin secretion from islet cells [10], zygote development [11,12], *N*-acetylaspartate (a myelin precursor) synthesis [13–16] and glial synthesis of glutamate and glutamine [17]. Increasing evidences support the hypothesis that MAS activity is crucial for breast cancer cell proliferation [18]. In this regard, it might divert energetic cell metabolism toward glycolysis, promoting cancer cell growth [19]. Furthermore, AGC is involved in taurine metabolism, since it can efficiently transport also cysteinesulfinate [4,20], an intermediate of cysteine degradation that serves as a precursor of taurine [21].

In *Homo sapiens,* two isoforms named AGC1 and AGC2 (also known as aralar and citrin) and encoded by the *SLC25A12* and *SLC25A13* genes, respectively, have been identified and characterized [4,22]. They belong to a subfamily of calcium-binding mitochondrial carrier sharing a characteristic bipartite structure, which consists of a C-terminal domain responsible for transport activity, and an N-terminal domain containing 8 EF-hands that regulates transport activity [4,23].

Aralar is mainly expressed in the heart, retina, skeletal muscle and brain [24,25], whereas citrin is widely expressed in the liver, epithelial cells and breast [4]. Aralar is involved in retinal visual function [26,27], in myelination process [13] and in glutamate-induced excitotoxicity [28,29]. Mutations in the *SLC25A12* gene have been found in autism spectrum disorders [25,30–32], as well as in a rare human disease (OMIM number 612949) implying developmental delay, epilepsy and hypotonia [15,33]. *SLC25A13* mutations are responsible for citrin deficiency that causes adult-onset type II citrullinemia (CTLN2, OMIM number 603471), neonatal intrahepatic cholestasis (NICCD, OMIM number 605814) [29,34–39], as well as failure to thrive and dyslipidemia caused by citrin deficiency (FTTDCD) [40].

In *D. melanogaster,* a single gene annotated in FlyBase as *CG2139* or *aralar1* encodes an ortholog of the human AGC isoforms [41]. A*ralar1* gene is involved in high energy demanding processes together with many other genes, such as those responsible for embryonic epithelial repair [42]. Previous studies indicated that *aralar1* locus is involved in the determination of bristle number in *D. melanogaster*, which are structures that may also have a neurosensory function [43], as well as this locus may influence wing size phenotype [44].

Differently from other fruit fly mitochondrial transporters, such as adenine nucleotide translocase [45], uncoupling protein [46,47], dicarboxylate [48], thiamine pyrophosphate [49,50], and glutamate carriers [51], a genomic analysis of this insect has highlighted the presence of a single gene (*CG2139*) encoding various *aralar1* spliced isoforms. The presence of so many alternatively spliced isoforms in mitochondrial carriers [47,52,53] and more in general in this organism is not surprising, since alternative splicing is a peculiar mechanism very often used by *D. melanogaster* to tightly control tissue- and stage-specific protein isoforms with different functions in development, as highlighted by Venables et co-workers *"Drosophila uses every alternative splicing strategy imaginable with an elegance and complexity that often eclipses mammals"* [54].

Despite the high metabolic relevance of this transporter, very few data are available on its biological role in fruit fly cellular processes, and no data at all are available on its transport properties in Drosophila.

In the present study, we have described (i) the expression profile of *D. melanogaster aralar1* gene in different developmental stages and tissues; (ii) the evolutionary changes that have shaped *aralar1* gene structure in arthropods; (iii) the functional characterization of recombinant Aralar1-PA and Aralar1-PE and their identification as the fruit fly mitochondrial aspartate/glutamate carriers.

2. Material and methods

2.1. Blast search of AGC orthologs in D. melanogaster and other species

The *D. melanogaster* ortholog of human AGCs was identified using the blastp algorithm (http://flybase.org/blast/). A BLAST search strategy, using *D. melanogaster* CDS and/or peptides as queries against genomic and ESTs databases, was also adopted to identify putative genes encoding AGC in the genome of other Drosophilidae and several non-Drosophilidae species [55]. A complete list of the species investigated in this study and the accession number in which *aralar1* genes have been identified is shown in Supplementary Table 1. These searches were performed using organism-specific (www.flybase.org,www.vectorbase.org and http://hymenopteragenome.org) and generalist genomic repositories (NCBI http://blast.ncbi.nlm.nih.gov/Blast.cgi). The "reciprocal best hit" approach was used to identify *aralar1* genes in different species. In this approach, a common evolutionary origin is supposed when in the compared genomes two gene sequences represent each other the best BLAST hit [56]. For each genomic sequence identified by using the above-mentioned criteria, exon/intron boundaries were carefully annotated after prediction *in silico* carried out with the aid of ESTs and cDNA sequences, if available, or predicted by the Genscan tool [57], or inferred by sequence similarity with transcript sequences of closely related species. Multiple alignments of amino acids, as well as coding and non-coding DNA sequences, were obtained using the MultAlin 5.4.1 software available at the MultAlin server (http://multalin.toulouse.inra.fr/multalin/) [58,59]. The matrix-scan pattern matching tool of the Regulatory Sequence Analysis Tools from the RSAT server (http://rsat.ulb.ac.be/) was used in combination with multiple alignments in order to identify Nuclear Respiratory Gene (NRG) elements [60] in the non-coding sequences of Drosophilidae and non-Drosophilidae *aralar1* genes.

2.2. Reverse-transcription analyses of aralar1 transcriptional isoforms

Oregon-R flies were raised on standard culture medium at 24 °C. Total RNA for gene expression analysis was achieved from 0.5 to 1 g samples of Oregon-R individuals at different developmental stages (embryo, larvae, pupae and adult flies). Except for ovaries and testes, male and female tissues equally contributed to each dissection. Total RNA from all the developmental stages and tissues was extracted by employing Trizol. Purified RNA was quantified using a Nanodrop spectrophotometer (Thermo Scientific) and diluted to 1 mg/ml for reverse transcription. RNA (1 μg) was reverse transcribed by employing the Quantitect reverse transcription kit (QIAGEN) [61,62] following the manifacturer's protocol. Amplification was carried out using the Platinum Taq DNA Polymerase (Thermo Fisher).

Primers used for amplification were:

aralar_RA_F ATTAGACGCGGGAATTGCTC
aralar_RA_R CTCCTCGTGAAAGTCGTGCAG
aralar_RB_F ATAGTGCGAACGTGCCTGA
aralar_RB_R ATGGCGAGATGAACCCAGTG
aralar_RC_F CCGATGCCAAGAATCTCCGT
aralar_RC_R TCCTCGTGAAAGTCGTGCAG
aralar_RE_F CAAATCACGCCGCTGGAGAT

aralar_RE_F GGCCCCTTTATCAAGCGCTA

2.3. Construction of the expression plasmids encoding D. melanogaster Aralar1 isoforms and mutants in E. coli and S. cerevisiae

The two protein isoforms Aralar1-PA and Aralar1-PE were considered for the functional characterization of *D. melanogaster CG2139* gene. Aralar1-RA and Aralar1-RE were amplified by polymerase chain reaction (PCR) from the cDNA of the fruit fly clones LD35441 and GH21613, respectively. Both clones were provided by Drosophila Genomics Resource Center (Indiana University 1001 East Third St., Bloomington IN, 47405–7107). The oligonucleotide primers (sense and antisense) used in PCR reactions carried suitable restriction sites at their 5′ ends for the further cloning of the amplified inserts in the pET-21b/V5-His *E. coli* expression vector [51]. The absence of a stop codon in the reverse primer sequence led to the expression of Aralar1 proteins containing V5/His-tag at their C-termini [63].

The WT Aralar1-RE cDNA was employed as a template to generate mutants named Δ5 (deletion from residue 301 to 305), Δ8 (deletion from residue 301 to 308), Δ12 (deletion from residue 299 to 310), and 5Ala (replacement of residues $K_{301}RRRK_{305}$ by consecutive alanines). All of the mutations were introduced by the overlap extension PCR method [64,65], using oligonucleotides with suitable mutations in their sequences. Primers used for amplification were:

aralar_PE_FTAGGAATTCACCAATGCACATCCCGTTTCC and
aralar_PE_R CGAAAGCTTGGATCCCGTGGCCGTCG for all mutants.

The following specific primers were used to generate the above-mentioned mutants:

aralar_PE_Δ5_F
CCATCAAGCAGGCTGGTGGATACCTCCGAGTAGCCGCA
aralar_PE_Δ5_R
TGCGGCTACTCGGAGGTATCCACCAGCCTGCTTGATGG.
aralar_PE_Δ8_F
CCATCAAGCAGGCTGGTGGAGTAGCCGCATCGACTATAGTGAC
aralar_PE_Δ8_R
GTCACTATAGTCGATGCGGCTACTCCACCAGCCTGCTTGATGG
aralar_PE_Δ12_F GCGCCGTCCATCAAGCAGGCCGCATCGACTATAGTGACCTGAGCAA
aralar_PE_Δ12_R TTGCTCAGGTCACTATAGTCGATGCGGCCTGCTTGATGGACGGCGC
aralar_PE_5Ala_F CCATCAAGCAGGCTGGTGGGCGGCTGCCGCAGCGATACCTCCGAGTAGCCGCA
aralar_RE_5Ala_R TGCGGCTACTCGGAGGTATCGCTGCGGCAGCCGCCCACCAGCCTGCTTGATGG

The aralar1-RA and aralar1-RE ORFs were recovered from pET-21b/V5-His clones by a *Eco*RI/*Age*I digestion and cloned in the modified yeast expression vector pYES2/V5-His [49], in which the inducible GAL1 promoter had been replaced with the constitutive TDH3 promoter. The frameshift of transcripts was avoided cloning a *Kpn*I/EcoRI fragment carrying the ATG start codon at ‘5-end. Fragments used were: GGTACCAGGATCCGATCTTGAACTGACTGAGATGGCGAATTC and GGTACCAGGATCCGATCTTGAACTGACTGAGATGGCGAATTC for aralar1-RA and for aralar1-RE, respectively.

2.4. Bacterial expression and purification of the recombinant proteins

Aralar1 proteins were overexpressed at high levels in *E. coli* BL21 (DE3) [49]. Their identities were assessed by MALDI-TOF MS of trypsin digests of the corresponding bands excised from a Coomassie blue-stained polyacrylamide gel [66,67]. Inclusion bodies were purified using sucrose density gradient centrifugation, next they were washed at 4 °C, firstly with TE buffer (10 mM Tris/HCl, 1 mM EDTA, pH 8), then twice with a buffer containing Triton X-114 (2%, *w/v*) and 10 mM HEPES (pH 8), and finally with 10 mM PIPES pH 6.5. Aralar1-PA and Aralar1-PE were solubilized in 2% sarkosyl (*w/v*), and a small residue was removed by centrifugation (258,000 *g*, 30 min). Solubilized proteins were diluted 10-fold with 10 mM PIPES pH 6.5 and reconstituted into liposomes [68].

2.5. Reconstitution into liposomes and transport assays

Reconstitution mixture (700 μl) contained 0.5–1 μg of solubilized proteins, Triton X-114 (1,3% w/v), L-α-phosphatidylcholine from egg yolk (1,3% w/v), as sonicated liposomes, 10 mM glutamate (except where otherwise indicated), and 20 mM PIPES at pH 6.5 [69]. These components were carefully blended, and the blend was recycled 13 times through the same Amberlite column (Bio-Rad) [69]. External substrate was eliminated from proteoliposomes on Sephadex G-75 columns, pre-equilibrated with 50 mM NaCl and 10 mM PIPES at pH 6.5. Transport at 25 °C was started by adding L-[^{14}C]glutamate (Scopus Research BV, Wageningen, Netherlands) at the indicated concentrations to substrate-loaded proteoliposomes (exchange reaction), or to empty proteoliposomes (uniport reaction). In both cases, transport was terminated by adding 30 mM pyridoxal phosphate (PLP). In control samples, inhibitor was added together with the external radioactive substrate based on the inhibitor stop method [70,71]. Finally, external substrate was removed and radioactivity into proteoliposomes was measured. The experimental values were adjusted by subtracting control values. The initial transport rate was measured from the radioactivity taken up by proteoliposomes after 1 min (in the initial linear range of substrate uptake). The free Ca^{2+} concentrations were determined fluorimetrically with fura-2-acetoxymethyl ester (Fura-2 AM) (Thermo Fischer Scientific). Fura-2 AM is a membrane-permeable, non-invasive derivative of the ratiometric calcium indicator fura-2. The excitation wavelengths used were 340 nm and 380 nm for Ca^{2+}-bound and Ca^{2+}-free fura-2 AM, respectively. In both states, the emission maximum was about 510 nm. The ratios 510 nm/340 nm and 510 nm/380 nm were directly related to the amount of Ca^{2+} [72]. Calcium dependence on transport activity was determined using de-ionized ultrapure water. In experiments for evaluating the influence of the membrane potential on the activity of the recombinant proteins, valinomycin was added to proteoliposomes in order to provide de-energized conditions. K^+ diffusion potentials were generated using valinomycin and K^+ gradients. In these experiments, substrate and buffer were neutralized with NaOH [4].

2.6. Yeast strains, growth conditions and functional complementation of yeast agc1Δ by Aralar1-PA and Aralar1-PE

W303 (wild-type) (*MATa {leu2–3112 trp1–1 can1–100 ura3–1 ade2–1 his3–11,15}*) yeast strain was provided by the EUROFAN resource center EUROSCARF (Frankfurt, Germany). The yeast AGC1 gene deletion (*agc*1Δ) and the cloning of endogenous yeast deleted gene AGC1 were achieved as described before [73].

The recombinant aralar1-RA-pYES2 and aralar1-RE-pYES2 plasmids were introduced into the *agc1*Δ yeast strain using the lithium acetate method [74], and transformants were selected on minimal medium lacking uracil supplemented with 2% glucose.

Functional complementation was achieved growing cells on liquid complete medium (1% Bacto yeast extract, 2% Bacto Peptone, pH 5.0) supplemented with 2% glucose (YPD) or 0.5 mM oleic acid dissolved in 10% Tween 40 (YPO) as carbon sources. Growths were started from medium log precultures grown on complete medium YPD and diluted with YPO to an optical density of 0.01 at 600 nm.

Simultaneously, washed cells were diluted and spotted on complete solid medium YPO, then plates were incubated for 72 h at 30 °C. Four-fold serial dilutions of both the transformed strains, wild-type and *agc1*Δ

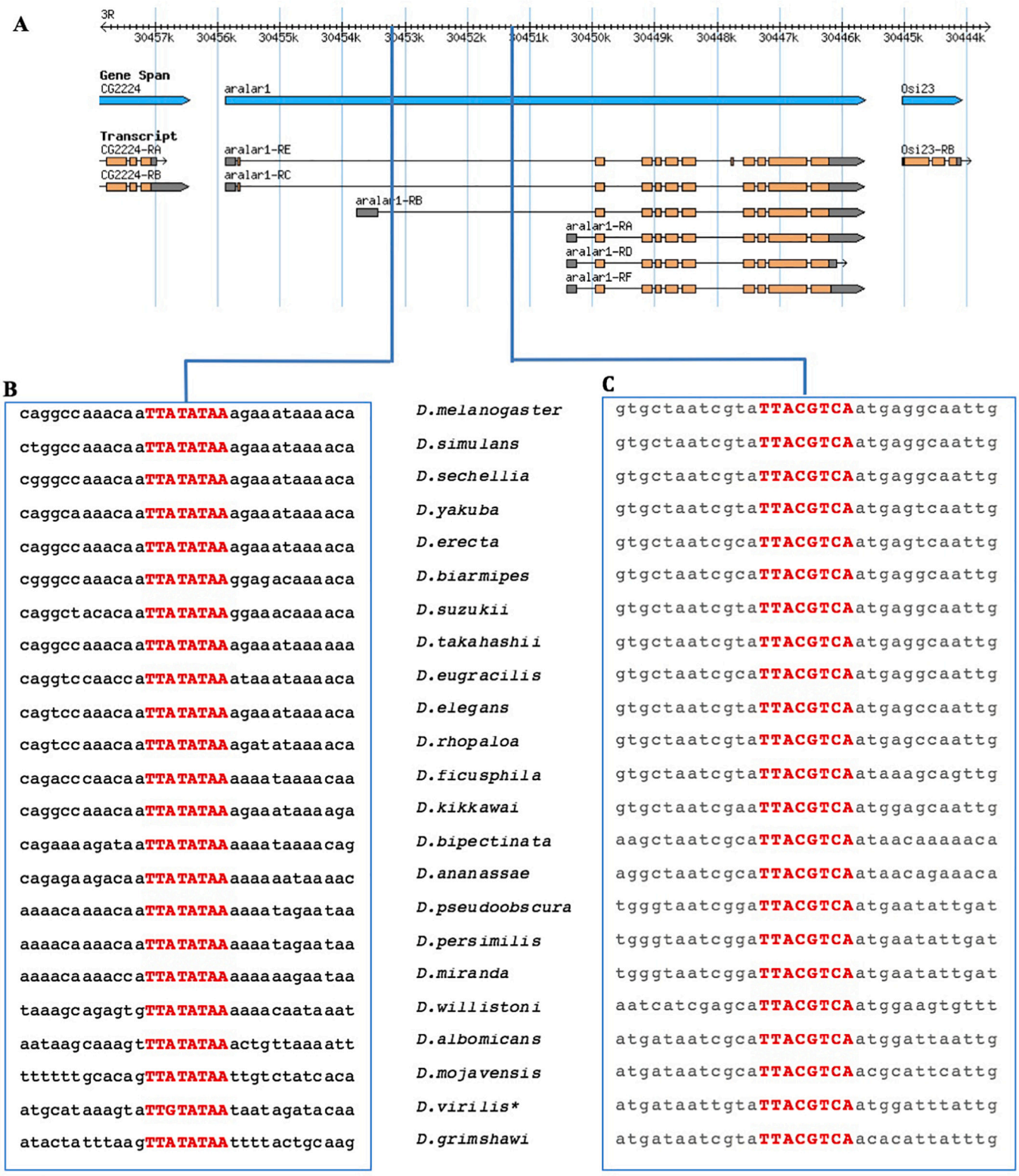

Fig. 1. Chromosomal organization of the *aralar1* gene in *D. melanogaster*. A) Overall organization of *aralar1* locus and its map position in *D. melanogaster*. B) and C) Multiple sequence alignments encompassing the two conserved NRG elements in the *aralar1* gene of 23 Drosophila species. * variant NRG motif in homologous position.

cells were analyzed.

2.7. Other methods

Proteins were resolved by SDS-PAGE and stained with Coomassie blue dye [75]. The amounts of recombinant pure Aralar1-PA and Aralar1-PE incorporated into liposomes were measured as previously described [76] and proved to be approximately 20% of the protein amount added to the reconstitution mixture. Moreover, recombinant proteins were resolved by SDS-PAGE analysis [77,78], then transferred to a nitrocellulose membrane and analyzed by Western blotting employing a mouse anti-V5 monoclonal antibody (Sigma-Aldrich) [79,80]. A multiple sequence alignment (MSA) of the fruit fly Aralar1 proteins, human aralar and citrin isoforms was obtained by using ClustalW to insert gaps in the MSA [81]. All data were analyzed using the statistical software GraphPad Prism Software (7.0 version). Pairwise comparisons between means of different groups were performed using a Student's *t*-test (two tailed, unpaired). Multiple comparisons were performed using a univariate ANOVA. Values at $P \leq 0.05$ were considered statistically significant, while values at $P \leq 0.01$ and $P < 0.001$ were considered very significant [82,83]. Orientation of functional Aralar-1 in the membrane of reconstituted proteoliposomes was investigated by ELISA assay performed as previously described [84]. ELISA tests were carried out on intact and permeabilized proteoliposomes by using either a rabbit polyclonal antiserum generated against 35–177 amino acids of Drosophila Aralar-1 proteins as described in [85] or an anti-V5 antibody directed against the V5 epitope placed at their C-termini (Sigma-Aldrich).

3. Results

3.1. Identification of genes encoding the aspartate/glutamate carrier in Drosophila species

A single gene, annotated in FlyBase as *CG2139* or *aralar1*, encodes a *D. melanogaster* ortholog of the human AGC isoforms (also known as aralar and citrin) [4], with no additional hits obtained throughout database mining. A*ralar1* locus spans roughly 10 Kbp on the third chromosome (3R:30,445,635…30,455,867 [-]) in the 99F4—99F5 cytogenetic band of polytene chromosomes of *D. melanogaster*. The transcriptional organization of *aralar1* reported in FlyBase (Fig. 1A) comprises six transcriptional isoforms. The utilization of alternative transcriptional start sites, alternative splicing and alternative UTRs, produces five different transcriptional isoforms (namely RA, RB, RC, RD, RE), which in turn can be translated into four different proteins (PA/PD, PB, PC, PE). An additional translational isoform is reported in FlyBase, Aralar1-PF, which is translated from the *aralar1-RF* transcript that is structurally identical to *aralar1-RA* isoform by mean of a read-through translational mechanism [86]. In this regard, *aralar1-RA* transcript is translated into a 682 amino acids long protein (Aralar1-PA), whereas *aralar1-RF* transcriptional isoform is translated into a polypeptide having 12 additional aminoacids at its C-terminus due to translation progression beyond the canonical stop codon. Three different promoters contribute to the transcription of *aralar1* locus. *Aralar1-RA* (identical to *aralar1-RF*) and *aralar1-RD* are transcribed from the same downstream promoter, with *aralar1-RD* transcript possessing a shorter 3'UTR if compared to that of *aralar1-RA/RF* isoforms. *Aralar1-RB* arises from the central promoter, whereas *aralar1-RC* and *aralar1-RE* are originated from the upstream promoter. The two latter isoforms differ by a short (36 bp long) exon, which is specifically incorporated into the *aralar1-RE* transcript. Given the availability of a wide range of sequenced Arthropoda genomes, we have surveyed *aralar1* gene structure in Arthropoda.

Orthologous genes in Drosophilidae have been retrieved using a BLAST strategy, and locus structure has been inferred with the aid of ESTs and cDNA sequences annotated in FlyBase and NCBI databases. Sequences with significant similarity to *D. melanogaster aralar1* gene have been detected in the genome of 22 additional Drosophila species (Supplementary Table 1), and their organization has been compared. Similarly to *D. melanogaster* annotation, in all the investigated Drosophila species three transcriptional start sites can be inferred from ESTs and cDNAs comparison and from inter-species similarity. In order to give a better snapshot of *aralar1* locus, its organization has been divided into three schemes highlighting the exon/intron organization relative to the three TSSs (Transcriptional Start Site) (Supplementary Tables 2–5). The comparison clearly suggests that the exon-intron structure of the locus is highly conserved in the 23 analyzed species. As can be observed, exon length is poorly variable. The first exon of all transcriptional isoforms is the most variable in length. Indeed, they encode the 5' UTRs and the leader peptides that are expected to be divergent in sequence, even if closely related species are compared. The length of the coding region of the last exon, encoding the protein C-terminus, also presents variable length and sequence in the analyzed Drosophila species. Internal coding exons are instead extremely conserved in length. As expected, introns are the most plastic regions of eukaryotic genes, and they are longer in species distantly related to *D. melanogaster*. It is worth to note that although the presence of the *aralar1-RE* specific exon is not supported by ESTs or cDNAs in the vast majority of the Drosophilidae species (not shown), it can be inferred by sequence similarity, suggesting that it could be also a functional exon in other species. In support of this hypothesis, the *aralar1-RE* specific exon, which can be 33–39 bp long depending upon the species, is flanked by a non-canonical donor splice site (GC) conserved in all the Drosophila species, suggesting the usage of an atypical splice site in the common ancestor of Drosophila and Sophophora genera (Supplementary Fig. 1).

3.2. Conservation of regulatory elements

Inter-species DNA sequence comparison is an excellent tool for the identification of cis-regulatory DNA sequences interested in eukaryotic gene expression regulation, especially in non-coding DNA sequence. In the noncoding sequences of Drosophilidae *aralar1* genes we have searched for conserved motifs by using phylogenetic footprinting and DNA pattern discovery softwares. The nuclear respiratory gene (NRG) element has been previously reported as a palindromic 8-bp motif (TTAYRTAA) that is shared by all nuclear OXPHOS genes [87], as well as by many other nuclear genes involved in biogenesis and function of mitochondria in insects [60]. In *D. melanogaster*, the NRG elements are usually located within an intron, in close proximity to the transcription start site (TSS), but it can be found in different gene locations, such as upstream the TSS. A NRG element (TTATATAA) associated with high weight and low *P* value in the RSAT output (8,2 and $6.0e^{-05}$ respectively) is located in the first intron, 518 bp downstream of the transcription start site related to *D. melanogaster aralar1-RB* transcriptional isoform. This 8-bp motif is extremely conserved and located in the first intron in all the Drosophilidae *aralar1* orthologs with high frequency (Fig. 1B). An additional NRG element, associated with a slightly lower score and a moderately higher *P*-value in the RSAT output (6,7 and $1,5e^{-04}$ respectively), is located downstream within the same intron, 686 bp upstream the TSS related to the RA/RD/RF transcriptional isoforms (Fig. 1C).

The functional importance of the NRG element in *aralar1* genes is suggested by its presence in the non-coding regions of *aralar1* genes belonging to the 32 non-Drosophilidae Arthropoda species investigated in this work (Supplementary Table 1). Notwithstanding the very long divergence times (divergence between Drosophila and Parasteatoda/Limulus genera is estimated approximately 600 MYA, from Treebase http://www.timetree.org) [88], single or multiple NRG elements have been detected in *aralar1* genes of the majority of Arthropoda species, and their intragenic localization is often strictly conserved (not shown). However, standing to the availability of transcriptional data in the vast majority of the studied cases, we have reconstructed the complete exon/intron structure of *aralar1* related to the shortest transcriptional isoform,

which we have arbitrarily assumed to be homologous to *D. melanogaster* RA-RD-RF transcripts. In many of these species, the NRG elements have been found in the first intron related to the shortest transcriptional isoform, suggesting that their positions could have been remodeled during insects' evolution. Also the length of the first intron, with respect to the most proximal TSS, is on average longer in non-Drosophilidae insects (mean length = 15,149 bp, 29 species) than in *D. melanogaster* homologs (mean length = 245 bp, 23 species), supporting the hypothesis of a functional role of the NRG elements, although in a different position.

3.3. All eukaryotic aralar1 genes have a common evolutionary origin

Sequences homologous to *D. melanogaster aralar1* gene have been found in the genomes of 23 Drosophilidae species. They share not only significant sequence similarity with *D. melanogaster* genes, but also a strikingly conserved exon/intron organization (Fig. 2 and Supplementary Tables 2–5). As a first step toward understanding the evolutionary history of *aralar1* genes, we have compared the Drosophilidae gene organization with their counterparts in an informative range of 32 Arthropod species consisting of 30 insects species (namely 7 Diptera, 2 Lepidoptera, 1 Coleoptera, 18 Hymenoptera and 2 Hemiptera), an Arachnida (*Parasteatoda tepidariorum*) and a Xiphosurida (*Limulus polyphemus*).

Similarly to what found in Drosophilidae, a single *aralar1* gene has been detected in the genome of all these species. The complete list of the identified *aralar1* genes and the accession numbers in which they have been found in the respective genomes is shown in Supplementary Table 1. Variations in the exon/intron organization of the investigated genes are reported in Supplementary Table 6. Comparison of all the investigated genes, in particular those in insects and Arachnida (*Parasteatoda tepidariorum*), as well as in Xiphosura (*Limulus polyphemus*), suggests the presence of a common ancestor before Arthropods'

Fig. 2. Eukaryotic AGC-encoding genes share an ancient intron-rich ancestor. The exon/intron structure of orthologous AGC-encoding genes of representative eukaryotic species is compared considering intron position, exon phase and length. Dashed lines indicate conservation of intron position. Translated AGC1-encoding regions are indicated in black, UTRs as white boxes. Internal *aralar1-RE* specific exons are indicated as grey boxes. Boxes are not in scale.

divergence. Intron loss seemingly occurred in Diptera-Lepidoptera-Coleoptera, while intron gain suggests a lineage-specific process.

The existence of an internal exon, specific for a transcriptional isoform homologous to *D. melanogaster aralar1-RE,* can be inferred in a subset of the analyzed species including Hymenoptera (14 out of 18 species) and Diptera (6 out of 7 non-Drosophilid species), whereas we have not detected it in Coleoptera (one species) and Lepidoptera (two species), as well as in the evolutionary distant Hemiptera species.

In humans, the nearly identical exon/intron organization of *ARALAR* (*SLC25A12*) and *CITRIN* (*SLC25A13*) genes (19 and 21 coding exons, respectively) is consistent with a duplication of an ancestral gene, which was probably present in the genome of the Vertebrate's ancestor, due to the existence of two paralogue genes in the genome of extant vertebrate species so far sequenced (not shown). Alternatively spliced transcript variants have been reported for the human *ARALAR* gene (as provided by ac.nos NM_003705, NR_047549, XM_011512070). While the NM_003705 is translated into the Aralar1 protein (NP_003696), the functional roles of the predicted (XM_011512070) and the putatively non-coding (NR_047549) transcriptional isoforms are currently unknown. Comparisons of exon phase, exon length, and intron positions, suggest that Arthropod and human genes have a unique intron-rich ancestor predating the divergence of such lineages. Since position conservation in humans and in numerous Arthropod lineages can be supposed in order to identify retained ancestral introns, we have deduced that such common ancestor gene contained at least 15 introns.

3.4. Expression pattern of Drosophila melanogaster aralar1 gene

The developmental expression pattern of *aralar1* in *D. melanogaster* is widely described in FlyBase, which reports the modENCODE mRNA-Seq temporal expression data (mRNA-Seq_U, [89]. Relative data are summarized in Fig. 3. In order to integrate these data with the expression pattern of *aralar1* transcriptional isoforms, we have carried out a Reverse Transcriptase-PCR analysis (RT-PCR) on total RNA samples isolated from distinct Drosophila developmental stages (Fig. 4A) or from dissected adult tissues (Fig. 4B).

With this aim, we have devised a set of primers specific to easily discriminate the five reported isoforms. Unfortunately, we were not able to find oligos suitable for performing quantitative analysis, so we could only conduct semiquantitative analyses based on RT-PCR. However, RA/RF and RD, cannot be distinguished, due to their nearly identical sequence, as described above. We will refer to *aralar1-RA* to indicate the RA/RD/RF isoforms through this paragraph.

The obtained results have revealed a constitutive expression of *aralar1-RA* transcript throughout development (Fig. 4A). By contrast, the expression of the other isoforms is patchy distributed during the development or in different tissues. *Aralar1-RB* isoforms are detected in early embryo development, during all the pupal stages and in adults, being only limited to females. Finally, *aralar1-RC* is detected in embryos (at least until 12–15 h after egg laying), in all the pupal stages and in both sexes during the adult stage, while *aralar1-RE* is expressed in the early-embryo development and in both sexes during the adult stage.

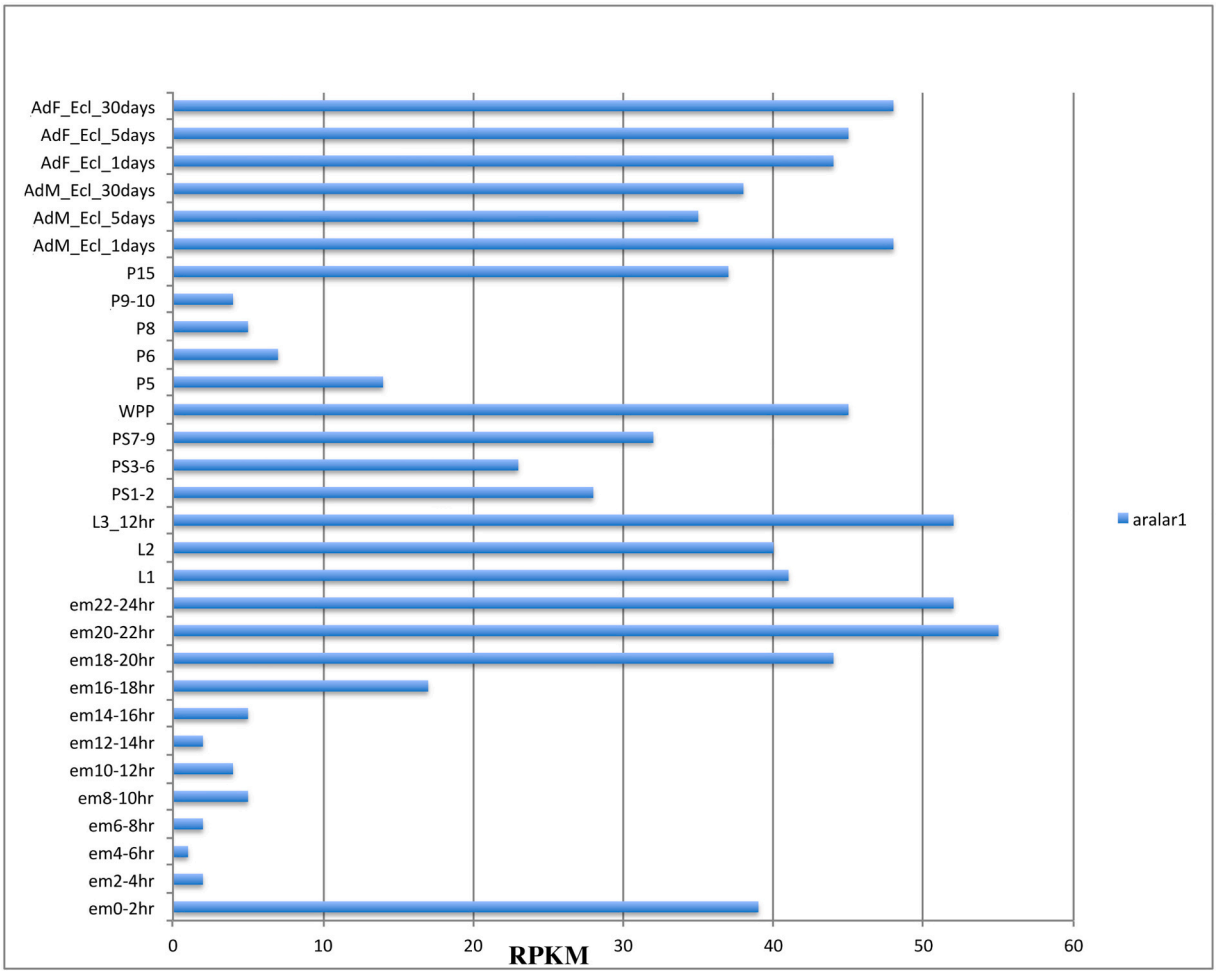

Fig. 3. modENCODE expression of *aralar1* through the development. Cumulative expression of all *aralar1* isoforms through the development is shown. Data were collected from modENCODE. Abbreviations legend. em: embryo stages; L: larval stages: P: pupae stages; AdM: adult males, various ages; AdF: adult females, various ages; RPKM: reads per kilobase million.

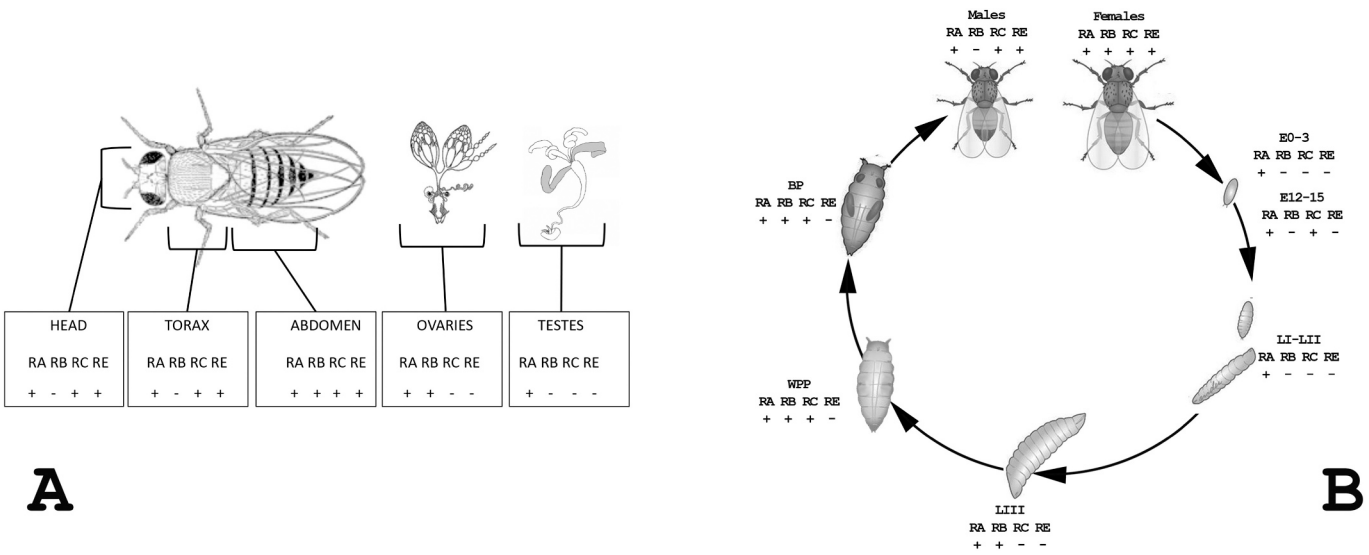

Fig. 4. Transcriptional analysis of *aralar1* in Drosophila adult tissues.
The presence/absence of the indicated *aralar1* isoforms revealed by the detection of RT-PCR fragment in each analyzed RNA sample is indicated with "+" or "–", respectively.
A) The impact of the four transcriptional isoforms of *aralar1* analyzed in adult heads, thoraces and abdomens, and in the reproductive organs of males and females of *D. melanogaster*. B) The presence/absence of four transcriptional isoforms of *aralar1* was analyzed by RT-PCR through development in the indicated stages. RNA samples were collected from embryos at two stages of embryonic development (0–3, 12–15 after egg lying), mixed first and second instar larvae (LI-LII), third instar larvae (LIII), white prepupae (WP), black pupae (BP), and adults (females and males).

Consistently with the expression pattern detected in whole adult males and females, we have found that *aralar1-RA*, *aralar1-RC* and *aralar1-RE* are ubiquitously expressed in all the main fruit fly body regions (namely head, thorax and abdomen), whereas *aralar1-RB* expression is limited to the abdomens of females, due to its ovary-specific expression (Fig. 4B).

3.5. Bacterial expression and functional characterization of recombinant Aralar1 proteins

A ClustalW alignment of Drosophila Aralar1 with the human AGC isoforms has revealed that all the proteins conserve the same domain structure organization consisting of an N-terminal domain with 8 EF-hands, a carrier domain and a C-terminal domain with unknown function (Fig. 5) [23]. Five out of the six Drosophila Aralar1 protein isoforms do not present any difference in their N-terminal EF-hands and carrier domains (Fig. 5). Aralar1-PE diverges from the other isoforms because of an insertion of 12 additional amino acid residues in the loop of its eighth EF-hand (EF-hand 8) [23]. In order to check if this peculiarity may affect its transport activity, we have chosen Aralar1-PE to be biochemically characterized together with Aralar1-PA that also shows a shorter N-terminus similar to that found in Aralar1-PD and Aralar1-PF (Fig. 5).

Aralar1-PA and Aralar1-PE have been overexpressed at high levels in *E. coli* BL21(DE3) (Fig. 6A, lane 3 for Aralar1-PA, lane 4 for Aralar1-PE). They have accumulated as inclusion bodies and have been purified by centrifugation on sucrose gradient and washing (Fig. 6A, lane 5 for Aralar1-PA, lane 6 for Aralar1-PE), with a yield of 50–60 mg/ml bacterial culture. These proteins have been not revealed in bacterial cells harvested just before the induction of expression (Fig. 6A, lane 1 for Aralar1-PA, lane 2 for Aralar1-PE), or in cells harvested after induction but do not carrying the coding sequence for Aralar1-PA and Aralar1-PE in the expression vector (data not shown). Their identities have been assessed by western blot analysis employing a mouse anti-V5 monoclonal antibody (Fig. 6A, lanes 1–6).

Aralar1-PA and Aralar1-PE have been functionally reconstituted into liposomes and the orientation of their N- and C-terminal regions in proteoliposomes was performed by ELISA assay, indicating that both termini of Aralar1 proteins reconstituted into the proteoliposomal membrane protrude toward the outside, which in intact proteoliposomes is the only side of the membrane accessible to antibodies (Supplementary Fig. 2). Aralar1-PA and Aralar1-PE transport activities have been tested in homo-exchange experiments (same substrate inside and outside). Using external and internal substrate concentrations of 1 and 10 mM, respectively, both proteins efficiently catalyze [^{14}C]glutamate/glutamate and [^{14}C]aspartate/aspartate exchange reactions. A very active uptake of [^{14}C]glutamate and [^{14}C]aspartate has also been observed when proteoliposomes had been preloaded with 10 mM aspartate or glutamate, respectively (hetero-exchange reactions). Both proteins do not catalyze any homo-exchange of phosphate, ADP, ATP, malonate, malate, oxoglutarate, ketoisocaproate, citrate, carnitine, ornithine, lysine, arginine, glutathione, choline, proline, and threonine (data not shown). No [^{14}C]glutamate/aspartate exchange has been observed using boiled Aralar1-PA and Aralar1-PE for incorporation into liposomes or reconstituting sarcosyl-solubilized bacterial material deriving either from cells not carrying any expression vector for Aralar1-PA and Aralar1-PE or from cells collected just before the induction of expression.

We have displayed kinetics of Aralar1-PA and Aralar1-PE uptake in Fig. 6B. Each protein reconstituted into proteoliposomes contains 10 mM internal glutamate, and uptake has been measured in the presence of external 0.5 mM [^{14}C]glutamate (exchange). Exchange reactions follow first-order kinetics, and isotopic equilibrium is approached exponentially, maximum uptake is reached after 90 min (rate constants 0.066 and 0.080 min^{-1} and initial rates of 20.78 and 59.51 nmol/min × mg protein for Aralar1-PA and Aralar1-PE, respectively). Conversely, no [^{14}C]glutamate uptake is observed in the absence of an internal substrate (uniport), highlighting that both proteins are unable to catalyze a unidirectional transport of glutamate (Fig. 6B). After 50 min incubation, when radioactive uptake by proteoliposomes has approached equilibrium, the addition of 20 mM unlabeled aspartate leads to an extensive efflux of radiolabeled glutamate from glutamate-loaded proteoliposomes (Fig. 6B). A similar efflux of labeled substrate is observed by adding 20 mM unlabeled glutamate (not shown). This efflux further confirms the strict exchange mechanism catalyzed by Aralar1-PA and Aralar1-PE. The unidirectional transport has been further investigated

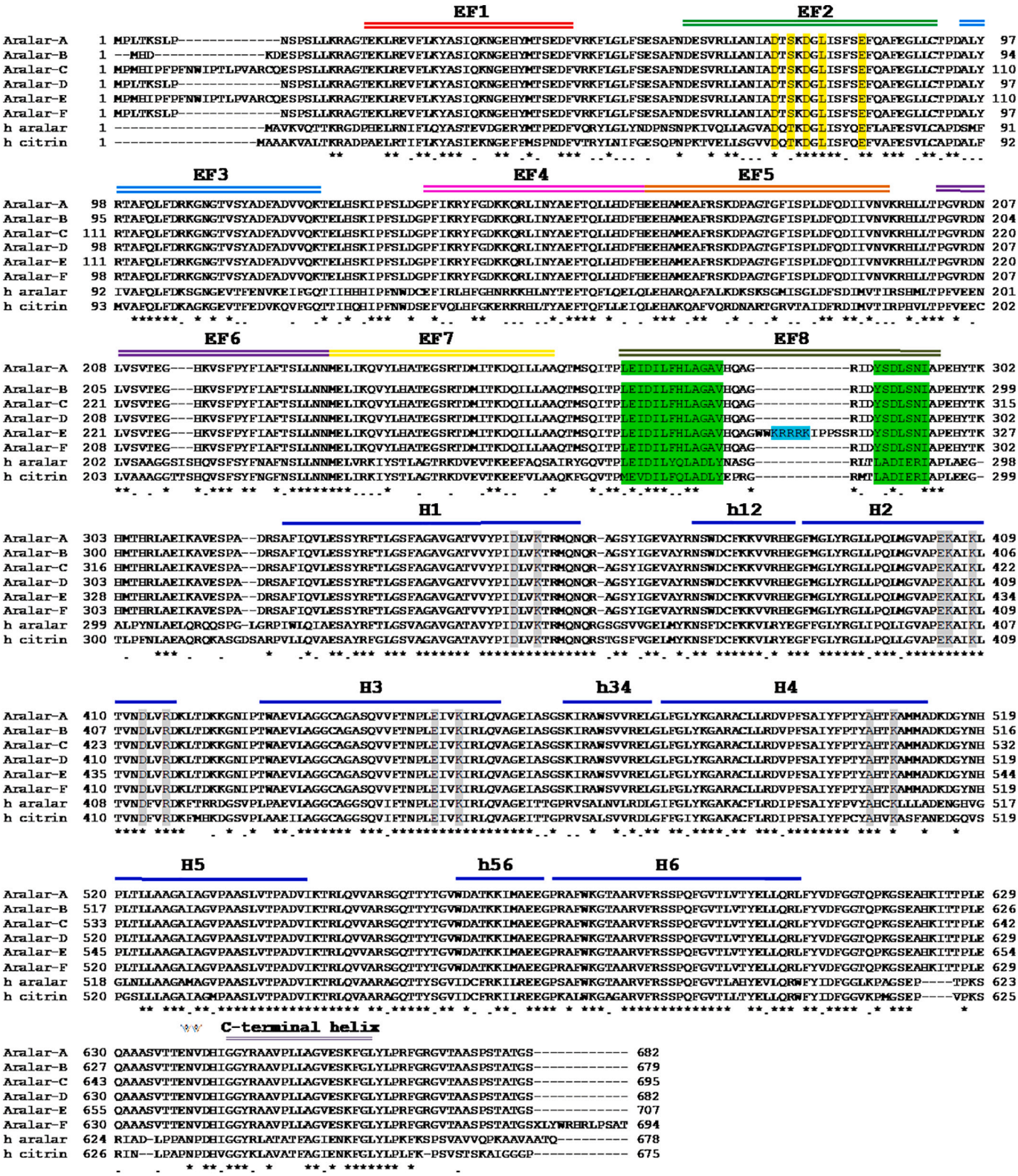

Fig. 5. Alignment of Drosophila Aralar1-PA-PF and human aralar and citrin. Sequence conservation is indicated with an asterisk for identical residues, a dot for conserved substitutions, and a gap for non-conserved residues. The EF-hands, the six transmembrane helices H1-H6, the three small helices parallel to the membrane plane h12-h56, and the C-terminal α-helix are indicated by coloured bars and labels. The two α-helices of EF-hand 8 and the positive residues in the loop of Aralar-1-PE are shaded in green and cyan, respectively. Residues that are involved in the coordination of calcium and the contact points of the substrate-binding site are shaded in yellow and grey, respectively. The alignment was obtained by using ClustalW. (For interpretation of the references to colour in this figure legend, the reader is referred to the web version of this article.)

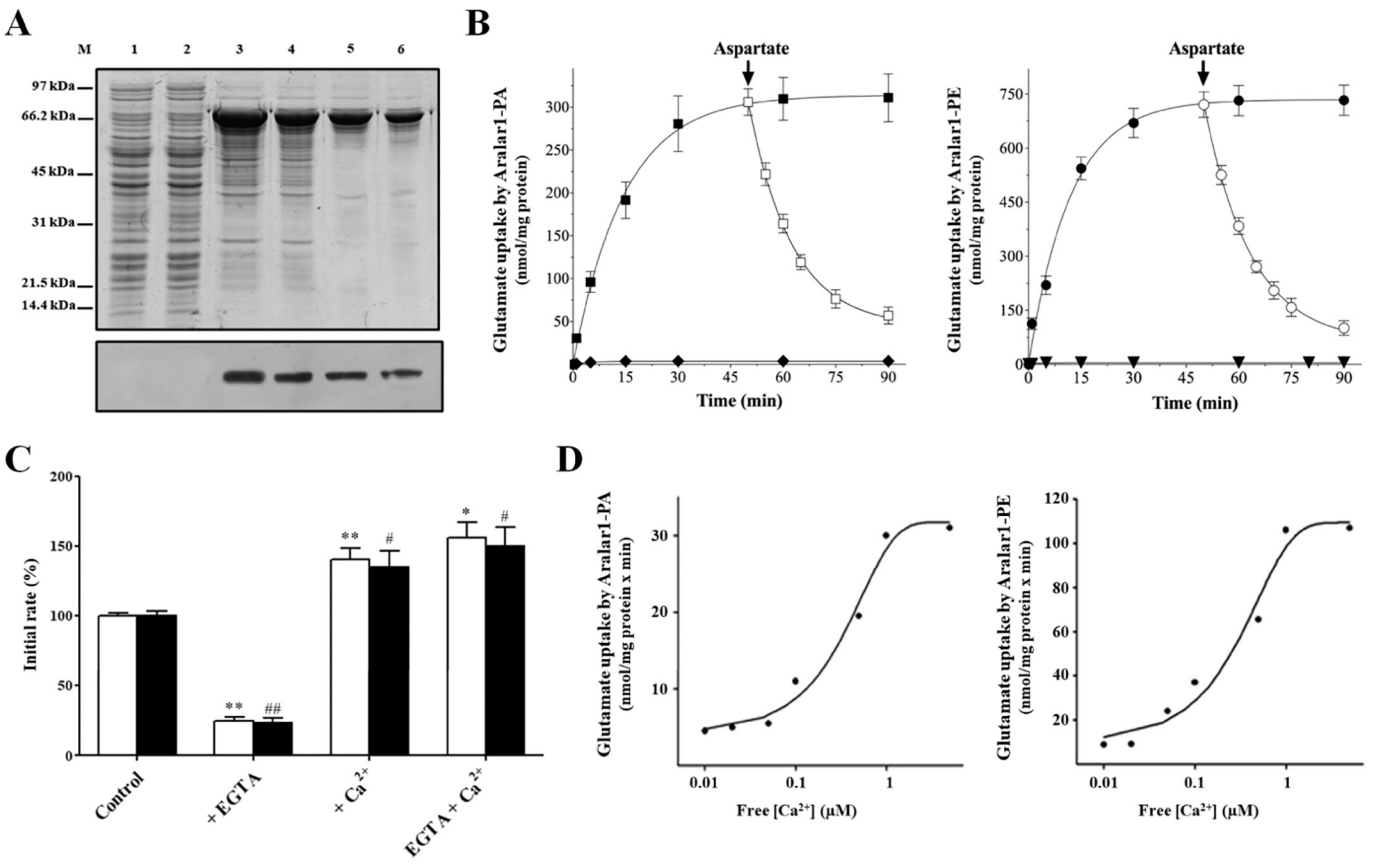

Fig. 6. Bacterial expression and functional characterization of Aralar1-PA and Aralar1-PE. (A) Expression in *Escherichia coli* of recombinant Aralar1. Proteins were separated by SDS-PAGE and stained with Coomassie blue dye or transferred to nitrocellulose and immunodetected with an anti-V5 monoclonal antibody. Lane M, markers; lanes 1–6, *E. coli* BL21(DE3) containing the expression vector with the coding sequence for Aralar1-PA (lanes 1, 3 and 5) and Aralar1-PE (lanes 2, 4 and 6). Samples were taken at the time of the induction (lanes 1 and 2) and 4 h later (lanes 3 and 4). Lanes 5 and 6, Aralar1-PA and Aralar1-PE originating from bacteria shown in lanes 3 and 4, respectively, purified by centrifugation on sucrose gradient. The same number of bacteria was analyzed in each sample. (B) Kinetics of [^{14}C] glutamate/glutamate exchange by Aralar1-PA and Aralar1-PE. Proteoliposomes were reconstituted with Aralar1-PA and Aralar1-PE. 0.5 mM [^{14}C]glutamate was added to proteoliposomes containing 10 mM glutamate (■ and ●) or 10 mM NaCl (◆ and ▼). When the uptake approached equilibrium (50 min), 20 mM of aspartate was added outside the proteoliposomes (□ and ○). Similar results were obtained in four independent experiments. (C–D) Effect of Ca^{2+} on transport activities of Aralar1-PA and Aralar1-PE. (C) Recombinant Aralar1-PA (open bars) and Aralar1-PE (filled bars), were reconstituted into proteoliposomes, [^{14}C]glutamate/glutamate transport rates were measured in de-ionized ultrapure water without additions (Control) or with the addition of 0.5 mM EGTA, or 1 mM $CaCl_2$, or 0.5 mM EGTA in the presence of 1 mM $CaCl_2$. Uptake rates of glutamate/glutamate exchange were measured at 60 s. Results are expressed as a percentage of the Aralar1-PA and Aralar1-PE values, which were on average 35.31 ± 1.24 and 110.58 ± 3.76 nmol/min × mg of protein, respectively. The average transport rates were calculated from the average of at least five independent experiments and displayed with the standard error. Different symbols indicate statistical differences, when occurring, between means of values as indicated by ANOVA. $^{*}P < 0.05$, $^{**}P < 0.01$ *vs* Aralar1-PA control, $^{\#}P < 0.05$, $^{\#\#}P < 0.01$ *vs* Aralar1-PE control). (D) Dependence of Aralar1-PA and Aralar1-PE activities on the free Ca^{2+} concentration. [^{14}C]glutamate transport rates were measured in de-ionized ultrapure water in the presence of 0.5 mM EGTA and various concentrations of Ca^{2+}. Similar results were obtained in at least three independent experiments. (For interpretation of the references to colour in this figure legend, the reader is referred to the web version of this article.)

in backward experiment, as it provides a more convenient assay [53], *i.e.*, by measuring the efflux of [^{14}C]glutamate from prelabeled active proteoliposomes; in the absence of an external substrate no efflux of [^{14}C]glutamate has been observed, even after 60 min of incubation, but an extensive efflux has occurred upon the addition of 10 mM external glutamate or aspartate (data not shown).

Substrate specificity of recombinant Aralar1-PA and Aralar1-PE has been examined in detail by measuring the uptake of [^{14}C]glutamate into proteoliposomes preloaded with different possible substrates. Table 1 reports the results of our explorative statistical analysis. Both proteins efficiently exchange external [^{14}C]glutamate for internal L-glutamate or L-aspartate. Aralar1-PA also catalyzes a lower but significant uptake of [^{14}C]glutamate in the presence of internal L-cysteinesulfinate, whereas no transport activity has been found with L-α-aminoadipate, L-glutamine and L-asparagine (Table 1). Differently from Aralar1-PA and yeast AGC [90], but similarly to the human AGC isoforms [4], Aralar1-PE exchanges external [^{14}C]glutamate for internal cysteinesulfinate at the same rate as aspartate, and it shows a significantly high [^{14}C]glutamate uptake in the presence of internal L-α-aminoadipate and L-glutamine. Both isoforms are virtually unable to exchange [^{14}C]glutamate for internal D-aspartate and D-glutamate, indicating a high degree of stereo specificity.

The [^{14}C]glutamate/glutamate exchange reactions catalized by Aralar1-PA and Aralar1-PE are hampered by many well-known inhibitors of several MCF members, being completely inhibited by 50 μM *p*-chloromercuribenzoate [4] and 1 mM pyrocarbonate [90] (100 and 96% inhibition, respectively for both proteins) and, to a slightly lesser extent by 50 μM mersalyl [76] and 0.1% tannic acid [53] (80 and 85% inhibition, respectively for both proteins), and also by 1 mM *N*-ethylmaleimide [53] (40 and 50% inhibition for Aralar1-PA and Aralar1-PE, respectively). Moreover, 10 mM bathophenanthroline or 0.1 mM bromocresol purple [53] are unable to exert a significant inhibition. Additionally, no inhibition has been observed with 10 μM bongkrekic acid [68] and 2.5 mM 1,2,3-benzenetricarboxylate [81], which are specific

Table 1
Dependence on internal substrate of the transport properties of proteoliposomes reconstituted with recombinant Aralar1-PA and Aralar1-PE.

Internal substrate	[^{14}C]Glutamate transport	
	Aralar1-PA	Aralar1-PE
	nmol/min × mg of protein	
None (Cl^- present)	1.63 ± 0.11	2.85 ± 0.19
L-Glutamate	31.27 ± 1.31***	105.5 ± 6.89###
L-Aspartate	23.14 ± 1.21***	63.34 ± 2.78###
L-Cysteinesulfinate	13.76 ± 0.78***	73.91 ± 3.23###
L-α-Aminoadipate	2.34 ± 0.13*	38.05 ± 2.98###
L-Glutamine	1.84 ± 0.16	14.68 ± 1.24###
L-Asparagine	3.63 ± 0.27*	9.51 ± 1.02#
D-Aspartate	1.65 ± 0.10	2.99 ± 0.22
D-Glutamate	1.34 ± 0.12	2.77 ± 0.25

Proteoliposomes were preloaded internally with various substrates (at 10 mM concentration). Transport was started by adding 0.5 mM [^{14}C]glutamate to proteoliposomes reconstituted with Aralar1-PA and Aralar1-PE, respectively, and terminated after 1 min. For each internal substrates four indipendent experiments have been carried out. The means and the standard deviations of Aralar1-PA and Aralar1-PE for each substrate are reported. Different symbols indicate statistical differences between means of values as indicated by ANOVA (*$P \leq 0.05$, ***$P \leq 0.001$ *vs* uniport reaction by Aralar1-PA, #P ≤ 0.05,##$P \leq$ 0.01, ###P ≤ 0.001 *vs* uniport reaction by Aralar1-PE).

inhibitors of the mitochondrial ADP/ATP and citrate carrier, respectively.

Considering that the AGC-catalyzed aspartate/glutamate antiport reaction is electrogenic [4], the effect of membrane potential has been examined on the aspartate/glutamate exchange reaction mediated by our Aralar1 carriers. A K^+diffusion potential has been created across the membrane of proteoliposomes using valinomycin/KCl (calculated value ~100 mV, positive inside). In such conditions, the rates of the [^{14}C] $aspartate_{out}$/$glutamate_{in}$ exchanges of Aralar1-PA and Aralar1-PE are stimulated (Table 2). In the absence of a membrane potential or when homo-exchanges have been measured, no effect has been observed. As a consequence, Aralar1-PA and Aralar1-PE are able to catalyze an electrogenic exchange of aspartate for glutamate.

We have determined the kinetic constants of the recombinant purified Aralar1-PA and Aralar1-PE by measuring the initial transport rate at various external [^{14}C]glutamate or [^{14}C]aspartate concentrations, in the presence of a constant internal saturating concentration (10 mM) of unlabeled substrates. In five independent experiments carried out at the same internal and external pH (6.5), the half-saturation constants (K_m) of reconstituted Aralar1-PA and Aralar1-PE for glutamate are 0.26 ± 0.03 and 0.29 ± 0.07 mM, respectively, and for aspartate are 47 ± 2.3 and 51 ± 2.6 μM, respectively. Interestingly, the two isoforms significantly differ in their V_{max} values, which are 32.25 ± 1.69 and 94.29 ± 5.40 nmol/min/mg protein, for Aralar1-PA and Aralar1-PE, respectively for both substrates. Activity has been normalized by determining the amount of recombinant proteins recovered into proteoliposomes after reconstitution. We have further analyzed whether the differences in transport rates (Table 1) and Vmax values found between the two isoforms could arise from the 12 additional amino acid residues present in the loop of the helix-loop-helix structure of the eighth EF-hand (EF-hand 8) of Aralar1-PE. First of all, we have checked, in de-ionized ultrapure water, the effect of Ca^{2+} or EGTA (a divalent ion chelator) on Aralar1-PA and Aralar1-PE transport activity (Fig. 6C). The activities of both isoforms are increased of about 35% by the addition of 1 mM $CaCl_2$ and diminished by the addition of 0.5 mM EGTA. The inhibitory effect of EGTA is abolished in the presence of 1 mM $CaCl_2$ (Fig. 6C). These results indicate that both isoforms are highly sensitive to calcium, since a low calcium contamination in the reconstitution mixture is able to activate transport activity of both isoforms, whereas its removal by a Ca^{2+} chelator exerts an inhibitory effect. The Ca^{2+}-dependence of the transport activities of Aralar1-PA and Aralar1-PE has been further studied by measuring their transport rates as a function of the free Ca^{2+} concentration (Fig. 6D). Both isoforms are highly Ca^{2+}-sensitive, since Aralar1-PA and Aralar1-PE have a half-maximal activation of about 0.34 and 0.15 μM, respectively.

3.6. Influence of the eighth EF-hand on the activity of Aralar1-PE isoform

Once established that in our recostituted system calcium is able to regulate transport activity of both isoforms, we have checked if the shortening of the insertion consisting of 12 additional residues in Aralar1-PE or the replacement of some residues might affect its transport activity. In particular, the five positive charged residues (KRRRK from 301 to 305) have been replaced by consecutive alanine residues (5Ala mutant) or deleted (Δ5 mutant). Two further deletions have also been investigated, the first encompassing residues 301–308 (Δ8 mutant), and the second including residues 299–310 (Δ12mutant); in this latter mutant the insertion characterizing Aralar1-PE has been completely removed. Substrate specificity of recombinant Aralar1-PE mutants has been examined in detail by measuring the uptake of [^{14}C]glutamate into proteoliposomes preloaded with different possible substrates. As reported in Fig. 7, the substitution of the five charged residues with Ala deeply increases transport activity of all the tested substrates, whereas its deletion decreases tranport activity proportionally with the size of the deletion gradually leading Aralar1-PE to have the same substrate specificity of Aralar1-PA. The kinetic constants of the recombinant Aralar1-PE mutants are reported in Table 3. The half-saturation constants (K_m) of reconstituted mutants do not vary with respect to the wild-type, whereas as regards transport activity a significant change has been observed. In particular, 5Ala mutant shows a transport activity three-fold higher than that of the wild-type protein, whereas deletions negatively affect transport activity, which decreases proportionally with the size of the deletion. Interestingly, Δ12 mutant exhibits the same transport activity as Aralar1-PA.

Table 2
Influence of the membrane potential on the activity of recombinant Aralar1-PA and Aralar1-PE.

Internal substrate	K^+_{in}/k^+_{out} (mM/mM)	[^{14}C]Aspartate uptake (*nmol/min × mg protein*)			
		Aralar1-PA		Aralar1-PE	
		−valinomycin	+ valinomycin	−valinomycin	+ valinomycin
Aspartate	1/1	28.75 ± 2.11	30.05 ± 2.96	100.75 ± 8.55	102.21 ± 8.40
	1/50	27.37 ± 2.41	28.64 ± 2.05	103.25 ± 7.20	103.89 ± 9.10
Glutamate	1/1	21.52 ± 1.70	22.24 ± 1.45	76.33 ± 5.88	77.14 ± 6.39
	1/50	23.95 ± 2.35	57.48 ± 5.74**	75.68 ± 6.28	154.86 ± 7.50**

Exchange was started by the addition of 50 μM [^{14}C]aspartate to proteoliposomes containing 10 mM of the indicated internal substrate. K^+_{in} was included as KCl in the reconstitution mixture, whereas K^+_{out} was added as KCl together with the labeled substrate. Differences in osmolarity were compensated for by the addition of appropriate concentrations of sucrose in the opposite compartment. Valinomycin (1.0 μg/mg phospholipid) was added in 10 μl ethanol/ml of proteoliposomes (+ valinomycin). In samples without valinomycin (− valinomycin) only ethanol was added. Exchange reactions were stopped after 1 min. Similar results were obtained in three independent experiments. Asterisks indicate values that are significantly different from those obtained in the same experiment but in the absence of valinomycin (**$P \leq 0.01$, using Student's *t*-test).

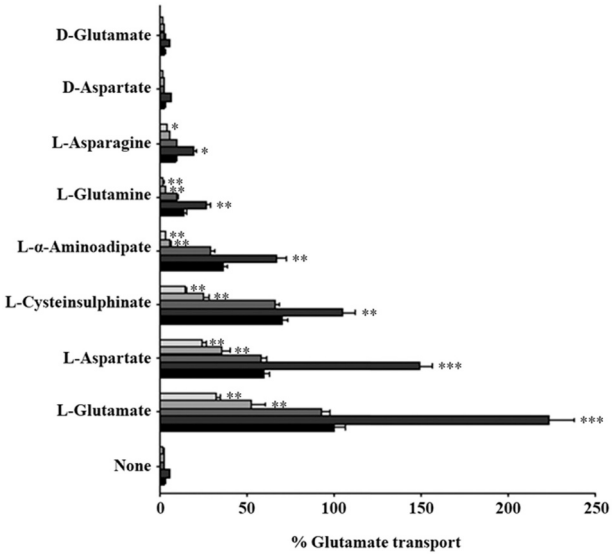

Fig. 7. Dependence on internal substrate of the transport properties of proteoliposomes reconstituted with recombinant Aralar1-PE, 5Ala, Δ5-Aralar1-PE, Δ8-Aralar1-PE and Δ12-Aralar1-PE mutants. Proteoliposomes reconstituted with Aralar1-PE (black bars), 5Ala (very dark grey bars), Δ5-Aralar1-PE (dark grey bars), Δ8-Aralar1-PE (light grey bars) and Δ12-Aralar1-PE (very light grey bars) were preloaded internally with various substrates (at 10 mM concentration). Transport was started by adding 0.5 mM [^{14}C]glutamate to proteoliposomes and terminated after 1 min. Data represent the mean of three independent experiments reported as the percent of glutamate transport with respect to the rate of [^{14}C]glutamate/glutamate exchange by Aralar1-PE (110 nmol/min/mg protein) setting at 100%. Asterisks indicate the level of statistical significance calculated comparing Aralar1-PE transport activity with that of its mutants in the presence of each internal substrate. *$P < 0.05$, **$P < 0.01$, ***$P < 0.001$, using ANOVA. (For interpretation of the references to colour in this figure legend, the reader is referred to the web version of this article.)

Table 3
Kinetic constants of recombinant Aralar1-PA, Aralar1-PE, 5Ala, Δ5-Aralar1-PE, Δ8-Aralar1-PE and Δ12-Aralar1-PE mutants.

Carrier	K_m (*mM*)	V_{max} (*nmol/min* × *mg protein*)
Aralar1-PA	0.26 ± 0.03	34.60 ± 2.11
Aralar1-PE	0.29 ± 0.07	92.08 ± 4.96
5Ala	0.31 ± 0.062	189.21 ± 10.50
Δ5-Aralar1-PE	0.33 ± 0.075	82.22 ± 7.55
Δ8-Aralar1-PE	0.31 ± 0.072	58.75 ± 5.10
Δ12-Aralar1-PE	0.30 ± 0.055	37.32 ± 3.15

The values were calculated from double reciprocal plots of the rate of [^{14}C] glutamate uptake *versus* substrate concentrations. Transport was started by adding 125–750 μM [^{14}C]glutamate to proteoliposomes containing 10 mM glutamate, and terminated after 1 min. Similar results were obtained in at least three independent experiments.

3.7. Aralar1-PA and Aralar1-PE function as an AGC transporter in S. cerevisiae

The yeast *AGC1* null mutant does not grow on oleate even in rich medium [90]. This phenotype is explained since MAS is required for reduction of the cytosolic NADH derived from peroxisomal oleate oxidation [90]. Thus, the expression of a mitochondrial carrier protein able to exchange aspartate with glutamate should abolish the growth defect of the *agc1*Δ knockout. Aralar1-PA and Aralar1-PE expressed in *AGC1* null cells have fully restored growth of the *agc1*Δ strain on oleate, similarly to the yeast Agc1p (Fig. 8), indicating that both Drosophila proteins function as AGC transporters. By contrast, in *agc1*Δ cells transformed with the empty vector no growth rescue has been observed.

4. Discussion

By allowing the mitochondrial re-oxidation of the cytosolic NADH, the MAS plays a central role in the redox homeostasis and in different metabolisms such as glucose homeostasis and nitrogen metabolism. The MAS requires the concerted functioning of six proteins, two located in the cytosol, the malate dehydrogenase 1 (MDH1) and the aspartate aminotransferase 1 (GOT1), two located in the mitochondrial matrix, the malate dehydrogenase 2 (MDH2) and the aspartate aminotransferase 2 (GOT2), and the last two located in the inner mitochondrial membrane, the aspartate/glutamate and the oxoglutarate/malate (OGC) carriers, which connect MAS cytosolic reactions to the mitochondrial ones. Despite the central role in energetic metabolism, very little is known about MAS components in the fruit fly, and up to date no functional data are available on AGC and OGC. In mammals, there are two genes encoding AGC, *ARALAR*, also known as AGC1, more widely expressed but absent in the liver, and *CITRIN* also known as AGC2, expressed in fewer tissues but present in the liver [24]. By searching the FlyBase database (http://flybase.org/) for human AGC homologs, we have found 6 alternatively spliced-isoforms annotated as *aralar1* and none as citrin.

The expression profile of *aralar1* transcriptional variants studied in this work suggests that three isoforms (namely *aralar1-RA/RF* and *aralar1-RD*) are constitutively transcribed throughout the development and in adult tissues. Due to their overlapping sequences, it is not possible to discriminate the expression profile of these transcriptional isoforms, which are transcribed from the innermost promoter. The slight differences observed in their organization suggest that they might have a different stability (*i.e.* half-life of their mRNA molecules) due to the length of the 3' UTR (*aralar1-RD* and *aralar1-RA* isoforms). Similarly, the stability of Aralar1-PF protein, encoded by *aralar1*-RF transcript (identical to *aralar1-RA* transcript), could be affected by the presence of the additional 12 amino acids introduced upon the translational read-through process [86].

Conversely, *aralar1-RB*, *aralar1-RC* and *aralar1-RE* transcriptional isoforms have a more complex expression pattern, as described in the Results section. While *aralar1-RB* is undetectable by RT-PCR in adult males, it can be specifically detected in adult ovary, suggesting its role in oogenesis. We do not know whether *aralar1-RB* detected during the early embryo development is the result of a maternal contribution or of the active transcription in embryos, as instead appears evident for *aralar1-RC* and *aralar1-RE*, which are undetectable in female germline and are present in early embryo developmental stages. Furthermore, while *aralar1-RC* expression persists in the whole adult tissues with the exclusion of the germline tissues, *aralar1-RE* expression is confined in the early stages of embryo development and in somatic adult tissues. The expression of the more active *aralar1-RE* in the early embryogenesis might be related to the very active aspartate and glutamate metabolism occurring in this stage [91]. *Aralar1-RB* and *aralar1-RC*, together with the constitutively expressed isoforms, seem to be also important during metamorphosis. It is noteworthy that all the *aralar1* transcriptional isoforms contribute to the strong *aralar1* expression observed in adult fat bodies (mainly located in the abdomen), as can be inferred by the combination of our results (see Fig. 4) and the modENCODE tissue expression data. Fat bodies are important energy storages and utilization organs in Drosophila, as well as in other insects [92], and they play a fundamental role in the post-metamorphic energy metabolism and egg development. Taken together, these results suggest that an isoform-specific expression pattern becomes defined after the initial embryo development, when all the isoforms are transcribed, and its establishment appears to be important for certain developmental stages or in specific adult tissues.

It can be speculated that the observed transcriptional pattern could be related to the presence of two evolutionary conserved DNA motifs, located between the TSSs of *aralar1-RB* and *aralar1-RA/RF/RD* transcripts. Although we have not performed functional studies aimed to

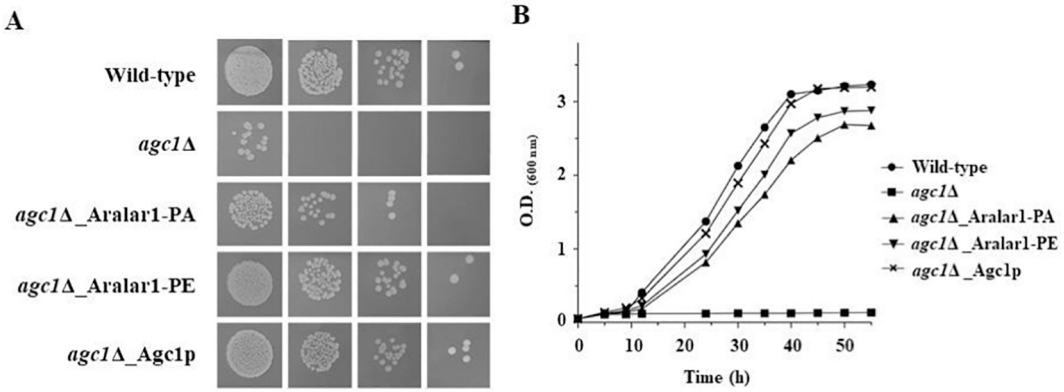

Fig. 8. Complementation of the growth defect of *agc1*Δ yeast strain by Aralar1-PA and Aralar1-PE. Wild-type, *agc1*Δ cells transformed with the empty vector (*agc1*Δ) and *agc1*Δ cells expressing drosophila Aralar1-PA, Aralar1-PE and yeast Agc1p were plated by using a four-fold serial dilution (A) or inoculated (B) in YP medium supplemented with 0.5 mM oleate. Plates and cell cultures were placed at 30 °C. Picture given in *A* was taken after 3 days to show yeast growth performance, whereas the optical density (*O.D.*) values at 600 nm given in *B* refer to cell cultures after the indicated growth times.

demonstrate their involvement in transcriptional regulation, it could be hypothesized that the NRG elements might influence *aralar1* gene expression for two reasons. Firstly, its evolutionary conservation in 23 Drosophila species belonging to two distinct sub-genera indicates a constrained role. Indeed, intron sequences are less conserved, even in related species, and only functionally constrained motifs are maintained. The divergence between *D. melanogaster* and *D. grimshawi* is thought to have occurred 50 Mya, and the conservation of such putative *cis*-acting sequence suggests a functional role. The NRG element can also be detected in non-Drosophilidae insects (Supplementary Table 6), thus enforcing its putative functional role, although its position related to the expressed transcriptional isoforms in these organisms is not easy to be determined.

Secondly, previous studies reported that the NRG elements are conserved in a subset of Drosophila genes encoding mitochondrial proteins, while they have been lost in duplicated genes, which in turn have acquired testis-specific transcription patterns. Since *alarar1* gene lacks paralogues in *D. melanogaster* (and in all the analyzed Drosophila species), the presence of two NRG elements within it might have acquired a different role, such as the establishment of a regulated expression pattern of all, or at least some, of the transcriptional *aralar1* isoforms. In this view, the two NRG elements detected could act either cooperatively or independently, as positive or negative regulators. Whether or not the two NRG elements are functional to *aralar1* expression cannot be determined without the aid of mutant or transgenic strains carrying *aralar1* genes containing disrupted NRG elements, which necessarily calls for future analyses.

In order to verify if this complex tissue- and developmental stage-specific transcriptional regulation is associated to the expression of functionally different isoforms, the transport properties of Aralar1-PA and Aralar1-PE, representing the two main encoded products of all *aralar1* transcripts, have been determined. The two recombinant proteins, once reconstituted into liposomes, catalyze a very efficient aspartate/glutamate electrogenic exchange reaction and are able to restore the yeast defect of the *AGC1* null gene (Fig. 8), confirming their identity as the *D. melanogaster* mitochondrial AGC. Similarly to the human isoforms [4], fruit fly Aralar1 isoforms do not show any significant difference in their substrate affinity, moreover, as the human isoforms, the Km value for aspartate was significantly lower than that for glutamate. Interestingly, although Aralar1-PA and Aralar1-PE differ only in their N-terminal halves, *i.e.*, region known to interact with calcium [23], they showed a significant different specific activity, being Aralar1-PE more active than Aralar1-PA. A similar situation had been previously found in *H. sapiens*, where citrin resulted more active than aralar [4].

Although fruit fly and human AGC isoforms showed this overlapping behavior, it should be emphasized that the different specific activities found in the latter are mainly due to their different carrier domains [4], whereas all *D. melanogaster* AGC isoforms share the same carrier domain and differ in their N-terminal domains. In fact, the recombinant carrier domain reconstituted into liposomes shows the same kinetic properties of Aralar1-PA (data not shown).

Interestingly, this N-terminal domain was also able to alter substrate specificity of the fruit fly AGC isoforms; since Aralar1-PE, similarly to human citrin [4], is able to exchange glutamate against cysteinesulfinate at the same rate as that of aspartate, while Aralar1-PA, similarly to human aralar, shows a glutamate/cysteinesulfinate exchange rate about one half lower than that of glutamate/aspartate. Furthermore, Aralar1-PE, differently from Aralar1-PA, significantly exchanges glutamate for L-α-aminoadipate and L-glutamine, suggesting a wider range of substrate specificity if compared to the latter.

A ClustalW alignment of Drosophila Aralar1 with human AGC isoforms has clarified that all proteins conserved the same structural organization including an N-terminal domain having 8 EF-hands with different functions (*i.e.* EF-hands 1–3 constitute a calcium-responsive unit, whereas EF-hands 4–8 are part of a static unit), a carrier domain and a C-terminal domain with unknown role (Fig. 5) [23]. Furthermore, calcium (EF-hands 1–3) and substrate binding sites are almost completely conserved between man and Drosophila, with a single conservative variation present in the calcium-binding site, where a threonine was replaced by a serine in the fruit fly isoforms (Fig. 5). The most variable regions in the fruit fly Aralar1 isoforms are located in the N-terminus and into the loop of the helix-loop-helix structure of EF-hand 8 (Fig. 5, green shaded) [23], where Aralar1-PE has an extra highly positive charged amino acid sequence. In the light of this observation, it is evident that N-terminus variations could play a fundamental role on the functional differences found between Aralar1-PA and Aralar1-PE. Site-direct mutagenesis experiments conducted on this additional region in EF-hand 8 have showed that the substitution of the charged residues by alanine can significantly affect substrate specificity and increase initial transport rate, whereas the progressive removal of these extra amino acids reduce initial transport rate and change substrate specificity until making Aralar1-PE similar to Aralar1-PA. Furthermore, this data are in agreement with the role proposed for the human AGC isoforms, in which the EF-hands 1–3 form a calcium-responsive mobile unit, EF-hands 4–8 form a static unit while the N-terminus region, external to the first EF-hand motif, seems not to be involved in any crucial regulatory function [23]. Finally, we have demonstrated that both proteins are Ca^{2+}-dependent, and similarly to citrin, Aralar1-PE shows a higher sensitivity to calcium being S0.5 about 2 times lower than that of Aralar1-PA.

Hence, biochemical characterization and calcium sensitivity have identified Aralar1-PA and Aralar1-PE as the human aralar and citrin counterparts, respectively (Fig. 6 C—D).

The functional characterization of the fruit fly mitochondrial AGC transporter represents a crucial step toward a complete understanding of the metabolic events acting during early embryogenesis, and it might strengthen the use of *D. melanogaster* as a model for genetics and developmental biology. Nevertheless, further studies of gain and loss of function are required to better understand how the complex transcriptional and expression patterns of Aralar1 regulates specific metabolic pathways in the different developmental stages of the fruit fly.

Supplementary data to this article can be found online at https://doi.org/10.1016/j.bbagen.2021.129854.

Credit author statement

Paola Lunetti: Conceptualization, Methodology, Formal analysis, Investigation, Writing - Original Draft, Writing - Review & Editing, Visualization. **René Massimiliano Marsano:** Methodology, Formal analysis, Investigation. **Rosita Curcio:** Conceptualization, Methodology, Formal analysis, Investigation, Writing - Original Draft, Writing - Review & Editing. **Vincenza Dolce:** Conceptualization, Methodology, Validation, Writing - Original Draft, Writing - Review & Editing, Supervision. **Giuseppe Fiermonte:** Validation, Data Curation, Funding acquisition. **Anna Rita Cappello:** Validation, Data Curation. **Federica Marra:** Investigation. **Roberta Moschetti:** Investigation. **Yuan Li:** Investigation. **Donatella Aiello:** Methodology, Investigation. **Araceli del Arco Martínez:** Methodology, Data Curation. **Graziantonio Lauria:** Methodology, Investigation. **Francesco De Leonardis:** Investigation. **Alessandra Ferramosca:** Validation, Data Curation. **Vincenzo Zara:** Validation, Project administration, Funding acquisition. **Loredana Capobianco:** Conceptualization, Methodology, Validation, Writing - Original Draft, Writing - Review & Editing, Supervision.

Declaration of Competing Interest

The authors declare that they have no known competing financial interests or personal relationships that could have appeared to influence the work reported in this paper.

Acknowledgements

This work was supported by Associazione Italiana per la Ricerca sul Cancro (FG grant n. 15404/2014); by the Italian Ministero dell'Istruzione, dell'Università e della Ricerca, MIUR, 2017PAB8EM_003; Drosophila clones were provided by Drosophila Genomics Resource Center NIH grant 2P40OD010949. The authors acknowledge "Sistema Integrato di Laboratori per L'Ambiente — SILA for providing lab tools.

References

[1] R. Curcio, P. Lunetti, V. Zara, A. Ferramosca, F. Marra, G. Fiermonte, A. R. Cappello, F. De Leonardis, L. Capobianco, V. Dolce, *Drosophila melanogaster* mitochondrial carriers: similarities and differences with the human carriers, Int. J. Mol. Sci. 21 (17) (2020).

[2] F. Palmieri, The mitochondrial transporter family SLC25: identification, properties and physiopathology, Mol. Asp. Med. 34 (2–3) (2013) 465–484.

[3] F. Palmieri, M. Monne, Discoveries, metabolic roles and diseases of mitochondrial carriers: a review, Biochim. Biophys. Acta 1863 (10) (2016) 2362–2378.

[4] L. Palmieri, B. Pardo, F.M. Lasorsa, A. del Arco, K. Kobayashi, M. Iijima, M. J. Runswick, J.E. Walker, T. Saheki, J. Satrustegui, F. Palmieri, Citrin and aralar1 are Ca(2+)-stimulated aspartate/glutamate transporters in mitochondria, EMBO J. 20 (18) (2001) 5060–5069.

[5] F. Palmieri, The mitochondrial transporter family (SLC25): physiological and pathological implications, Pflugers Arch. 447 (5) (2004) 689–709.

[6] B. Pardo, L. Contreras, A. Serrano, M. Ramos, K. Kobayashi, M. Iijima, T. Saheki, J. Satrustegui, Essential role of aralar in the transduction of small Ca2+ signals to neuronal mitochondria, J. Biol. Chem. 281 (2) (2006) 1039–1047.

[7] F.M. Lasorsa, P. Pinton, L. Palmieri, G. Fiermonte, R. Rizzuto, F. Palmieri, Recombinant expression of the Ca(2+)-sensitive aspartate/glutamate carrier increases mitochondrial ATP production in agonist-stimulated Chinese hamster ovary cells, J. Biol. Chem. 278 (40) (2003) 38686–38692.

[8] F.N. Gellerich, Z. Gizatullina, O. Arandarcikaite, D. Jerzembek, S. Vielhaber, E. Seppet, F. Striggow, Extramitochondrial Ca2+ in the nanomolar range regulates glutamate-dependent oxidative phosphorylation on demand, PLoS One 4 (12) (2009), e8181.

[9] I. Llorente-Folch, C.B. Rueda, I. Amigo, A. del Arco, T. Saheki, B. Pardo, J. Satrustegui, Calcium-regulation of mitochondrial respiration maintains ATP homeostasis and requires ARALAR/AGC1-malate aspartate shuttle in intact cortical neurons, J. Neurosci. 33 (35) (2013) 13957–13971 (13971a).

[10] B. Rubi, A. del Arco, C. Bartley, J. Satrustegui, P. Maechler, The malate-aspartate NADH shuttle member Aralar1 determines glucose metabolic fate, mitochondrial activity, and insulin secretion in beta cells, J. Biol. Chem. 279 (53) (2004) 55659–55666.

[11] M. Lane, D.K. Gardner, Mitochondrial malate-aspartate shuttle regulates mouse embryo nutrient consumption, J. Biol. Chem. 280 (18) (2005) 18361–18367.

[12] N. Moscatelli, P. Lunetti, C. Braccia, A. Armirotti, F. Pisanello, M. De Vittorio, V. Zara, A. Ferramosca, Comparative proteomic analysis of proteins involved in bioenergetics pathways associated with human sperm motility, Int. J. Mol. Sci. 20 (12) (2019).

[13] M. Ramos, B. Pardo, I. Llorente-Folch, T. Saheki, A. Del Arco, J. Satrustegui, Deficiency of the mitochondrial transporter of aspartate/glutamate aralar/AGC1 causes hypomyelination and neuronal defects unrelated to myelin deficits in mouse brain, J. Neurosci. Res. 89 (12) (2011) 2008–2017.

[14] E. Profilo, L.E. Pena-Altamira, M. Corricelli, A. Castegna, A. Danese, G. Agrimi, S. Petralla, G. Giannuzzi, V. Porcelli, L. Sbano, C. Viscomi, F. Massenzio, E. M. Palmieri, C. Giorgi, G. Fiermonte, M. Virgili, L. Palmieri, M. Zeviani, P. Pinton, B. Monti, F. Palmieri, F.M. Lasorsa, Down-regulation of the mitochondrial aspartate-glutamate carrier isoform 1 AGC1 inhibits proliferation and N-acetylaspartate synthesis in Neuro2A cells, Biochim. Biophys. Acta 1863 (6) (2017) 1422–1435.

[15] R. Wibom, F.M. Lasorsa, V. Tohonen, M. Barbaro, F.H. Sterky, T. Kucinski, K. Naess, M. Jonsson, C.L. Pierri, F. Palmieri, A. Wedell, AGC1 deficiency associated with global cerebral hypomyelination, N. Engl. J. Med. 361 (5) (2009) 489–495.

[16] M.A. Jalil, L. Begum, L. Contreras, B. Pardo, M. Iijima, M.X. Li, M. Ramos, P. Marmol, M. Horiuchi, K. Shimotsu, S. Nakagawa, A. Okubo, M. Sameshima, Y. Isashiki, A. Del Arco, K. Kobayashi, J. Satrustegui, T. Saheki, Reduced N-acetylaspartate levels in mice lacking aralar, a brain- and muscle-type mitochondrial aspartate-glutamate carrier, J. Biol. Chem. 280 (35) (2005) 31333–31339.

[17] B. Pardo, L. Contreras, J. Satrustegui, De novo synthesis of glial glutamate and glutamine in young mice requires aspartate provided by the neuronal mitochondrial aspartate-glutamate carrier Aralar/AGC1, Front. Endocrinol. 4 (2013) 149.

[18] J.M. Thornburg, K.K. Nelson, B.F. Clem, A.N. Lane, S. Arumugam, A. Simmons, J. W. Eaton, S. Telang, J. Chesney, Targeting aspartate aminotransferase in breast cancer, Breast Cancer Res. 10 (5) (2008) R84.

[19] C. Wang, H. Chen, M. Zhang, J. Zhang, X. Wei, W. Ying, Malate-aspartate shuttle inhibitor aminooxyacetic acid leads to decreased intracellular ATP levels and altered cell cycle of C6 glioma cells by inhibiting glycolysis, Cancer Lett. 378 (1) (2016) 1–7.

[20] F. Palmieri, I. Stipani, V. Iacobazzi, The transport of L-cysteinesulfinate in rat liver mitochondria, Biochim. Biophys. Acta 555 (3) (1979) 531–546.

[21] T. Ubuka, A. Okada, H. Nakamura, Production of hypotaurine from L-cysteinesulfinate by rat liver mitochondria, Amino Acids 35 (1) (2008) 53–58.

[22] K. Kobayashi, D.S. Sinasac, M. Iijima, A.P. Boright, L. Begum, J.R. Lee, T. Yasuda, S. Ikeda, R. Hirano, H. Terazono, M.A. Crackower, I. Kondo, L.C. Tsui, S. W. Scherer, T. Saheki, The gene mutated in adult-onset type II citrullinaemia encodes a putative mitochondrial carrier protein, Nat. Genet. 22 (2) (1999) 159–163.

[23] C. Thangaratnarajah, J.J. Ruprecht, E.R. Kunji, Calcium-induced conformational changes of the regulatory domain of human mitochondrial aspartate/glutamate carriers, Nat. Commun. 5 (2014) 5491.

[24] A. del Arco, J. Morcillo, J.R. Martinez-Morales, C. Galian, V. Martos, P. Bovolenta, J. Satrustegui, Expression of the aspartate/glutamate mitochondrial carriers aralar1 and citrin during development and in adult rat tissues, Eur. J. Biochem. 269 (13) (2002) 3313–3320.

[25] J. Liu, A. Yang, Q. Zhang, G. Yang, W. Yang, H. Lei, J. Quan, F. Qu, M. Wang, Z. Zhang, K. Yu, Association between genetic variants in SLC25A12 and risk of autism spectrum disorders: an integrated meta-analysis, Am. J. Med. Genet. B 168B (4) (2015) 236–246.

[26] J. Du, A. Rountree, W.M. Cleghorn, L. Contreras, K.J. Lindsay, M. Sadilek, H. Gu, D. Djukovic, D. Raftery, J. Satrustegui, M. Kanow, L. Chan, S.H. Tsang, I.R. Sweet, J.B. Hurley, Phototransduction influences metabolic flux and nucleotide metabolism in mouse retina, J. Biol. Chem. 291 (9) (2016) 4698–4710.

[27] L. Contreras, L. Ramirez, J. Du, J.B. Hurley, J. Satrustegui, P. de la Villa, Deficient glucose and glutamine metabolism in Aralar/AGC1/Slc25a12 knockout mice contributes to altered visual function, Mol. Vis. 22 (2016) 1198–1212.

[28] I. Llorente-Folch, C.B. Rueda, I. Perez-Liebana, J. Satrustegui, B. Pardo, L-Lactate-mediated neuroprotection against glutamate-induced excitotoxicity requires ARALAR/AGC1, J. Neurosci. 36 (16) (2016) 4443–4456.

[29] C.B. Rueda, I. Llorente-Folch, J. Traba, I. Amigo, P. Gonzalez-Sanchez, L. Contreras, I. Juaristi, P. Martinez-Valero, B. Pardo, A. Del Arco, J. Satrustegui, Glutamate excitotoxicity and Ca2+−regulation of respiration: role of the Ca2+

activated mitochondrial transporters (CaMCs), Biochim. Biophys. Acta 1857 (8) (2016) 1158–1166.
[30] L. Palmieri, V. Papaleo, V. Porcelli, P. Scarcia, L. Gaita, R. Sacco, J. Hager, F. Rousseau, P. Curatolo, B. Manzi, R. Militerni, C. Bravaccio, S. Trillo, C. Schneider, R. Melmed, M. Elia, C. Lenti, M. Saccani, T. Pascucci, S. Puglisi-Allegra, K.L. Reichelt, A.M. Persico, Altered calcium homeostasis in autism-spectrum disorders: evidence from biochemical and genetic studies of the mitochondrial aspartate/glutamate carrier AGC1, Mol. Psychiatry 15 (1) (2010) 38–52.
[31] N. Ramoz, J.G. Reichert, C.J. Smith, J.M. Silverman, I.N. Bespalova, K.L. Davis, J. D. Buxbaum, Linkage and association of the mitochondrial aspartate/glutamate carrier SLC25A12 gene with autism, Am. J. Psychiatry 161 (4) (2004) 662–669.
[32] J.A. Turunen, K. Rehnstrom, H. Kilpinen, M. Kuokkanen, E. Kempas, T. Ylisaukko-Oja, Mitochondrial aspartate/glutamate carrier SLC25A12 gene is associated with autism, Autism Res. 1 (3) (2008) 189–192.
[33] M.J. Falk, D. Li, X. Gai, E. McCormick, E. Place, F.M. Lasorsa, F.G. Otieno, C. Hou, C.E. Kim, N. Abdel-Magid, L. Vazquez, F.D. Mentch, R. Chiavacci, J. Liang, X. Liu, H. Jiang, G. Giannuzzi, E.D. Marsh, Y. Guo, L. Tian, F. Palmieri, H. Hakonarson, Erratum to: AGC1 deficiency causes infantile epilepsy, abnormal myelination, and reduced N-acetylaspartate, JIMD Rep. 14 (2014) 119.
[34] T. Saheki, K. Kobayashi, M. Iijima, M. Horiuchi, L. Begum, M.A. Jalil, M.X. Li, Y. B. Lu, M. Ushikai, A. Tabata, M. Moriyama, K.J. Hsiao, Y. Yang, Adult-onset type II citrullinemia and idiopathic neonatal hepatitis caused by citrin deficiency: involvement of the aspartate glutamate carrier for urea synthesis and maintenance of the urea cycle, Mol. Genet. Metab. 81 (Suppl. 1) (2004) S20–S26.
[35] Z.H. Zhang, Z.G. Yang, F.P. Chen, A. Kikuchi, Z.H. Liu, L.Z. Kuang, W.M. Li, Y. Z. Song, S. Kure, T. Saheki, Screening for five prevalent mutations of SLC25A13 gene in Guangdong, China: a molecular epidemiologic survey of citrin deficiency, Tohoku J. Exp. Med. 233 (4) (2014) 275–281.
[36] Y.Z. Song, Z.H. Zhang, W.X. Lin, X.J. Zhao, M. Deng, Y.L. Ma, L. Guo, F.P. Chen, X. L. Long, X.L. He, Y. Sunada, S. Soneda, A. Nakatomi, S. Dateki, L.H. Ngu, K. Kobayashi, T. Saheki, SLC25A13 gene analysis in citrin deficiency: sixteen novel mutations in east Asian patients, and the mutation distribution in a large pediatric cohort in China, PLoS One 8 (9) (2013), e74544.
[37] Y.Z. Song, M. Deng, F.P. Chen, F. Wen, L. Guo, S.L. Cao, J. Gong, H. Xu, G.Y. Jiang, L. Zhong, K. Kobayashi, T. Saheki, Z.N. Wang, Genotypic and phenotypic features of citrin deficiency: five-year experience in a Chinese pediatric center, Int. J. Mol. Med. 28 (1) (2011) 33–40.
[38] G. Fiermonte, G. Parisi, D. Martinelli, F. De Leonardis, G. Torre, C.L. Pierri, A. Saccari, F.M. Lasorsa, A. Vozza, F. Palmieri, C. Dionisi-Vici, A new Caucasian case of neonatal intrahepatic cholestasis caused by citrin deficiency (NICCD): a clinical, molecular, and functional study, Mol. Genet. Metab. 104 (4) (2011) 501–506.
[39] G. Fiermonte, D. Soon, A. Chaudhuri, E. Paradies, P.J. Lee, S. Krywawych, F. Palmieri, R.H. Lachmann, An adult with type 2 citrullinemia presenting in Europe, N. Engl. J. Med. 358 (13) (2008) 1408–1409.
[40] T. Saheki, Y.Z. Song, Citrin deficiency, in: M.P. Adam, H.H. Ardinger, R.A. Pagon, S.E. Wallace, L.J.H. Bean, K. Stephens, A. Amemiya (Eds.), GeneReviews((R)), Seattle (WA), 1993.
[41] A. Del Arco, M. Agudo, J. Satrustegui, Characterization of a second member of the subfamily of calcium-binding mitochondrial carriers expressed in human non-excitable tissues, Biochem. J. 345 (Pt 3) (2000) 725–732.
[42] I. Campos, J.A. Geiger, A.C. Santos, V. Carlos, A. Jacinto, Genetic screen in *Drosophila melanogaster* uncovers a novel set of genes required for embryonic epithelial repair, Genetics 184 (1) (2010) 129–140.
[43] C.L. Dilda, T.F. Mackay, The genetic architecture of Drosophila sensory bristle number, Genetics 162 (4) (2002) 1655–1674.
[44] H. Okada, H.A. Ebhardt, S.C. Vonesch, R. Aebersold, E. Hafen, Proteome-wide association studies identify biochemical modules associated with a wing-size phenotype in *Drosophila melanogaster*, Nat. Commun. 7 (2016) 12649.
[45] M.D. Brand, J.L. Pakay, A. Ocloo, J. Kokoszka, D.C. Wallace, P.S. Brookes, E. J. Cornwall, The basal proton conductance of mitochondria depends on adenine nucleotide translocase content, Biochem. J. 392 (Pt 2) (2005) 353–362.
[46] I.M. Sokolova, E.P. Sokolov, Evolution of mitochondrial uncoupling proteins: novel invertebrate UCP homologues suggest early evolutionary divergence of the UCP family, FEBS Lett. 579 (2) (2005) 313–317.
[47] M. Ulgherait, A. Chen, S.F. McAllister, H.X. Kim, R. Delventhal, C.R. Wayne, C. J. Garcia, Y. Recinos, M. Oliva, J.C. Canman, M. Picard, E. Owusu-Ansah, M. Shirasu-Hiza, Circadian regulation of mitochondrial uncoupling and lifespan, Nat. Commun. 11 (1) (2020) 1927.
[48] D. Iacopetta, M. Madeo, G. Tasco, C. Carrisi, R. Curcio, E. Martello, R. Casadio, L. Capobianco, V. Dolce, A novel subfamily of mitochondrial dicarboxylate carriers from *Drosophila melanogaster*: biochemical and computational studies, Biochim. Biophys. Acta 1807 (3) (2011) 251–261.
[49] D. Iacopetta, C. Carrisi, G. De Filippis, V.M. Calcagnile, A.R. Cappello, A. Chimento, R. Curcio, A. Santoro, A. Vozza, V. Dolce, F. Palmieri, L. Capobianco, The biochemical properties of the mitochondrial thiamine pyrophosphate carrier from *Drosophila melanogaster*, FEBS J. 277 (5) (2010) 1172–1181.
[50] C. Carrisi, D. Antonucci, P. Lunetti, D. Migoni, C.R. Girelli, V. Dolce, F.P. Fanizzi, M. Benedetti, L. Capobianco, Transport of platinum bonded nucleotides into proteoliposomes, mediated by *Drosophila melanogaster* thiamine pyrophosphate carrier protein (DmTpc1), J Inorg Biochem 130 (2014) 28–31.
[51] P. Lunetti, A.R. Cappello, R.M. Marsano, C.L. Pierri, C. Carrisi, E. Martello, C. Caggese, V. Dolce, L. Capobianco, Mitochondrial glutamate carriers from *Drosophila melanogaster*: biochemical, evolutionary and modeling studies, Biochim. Biophys. Acta 1827 (10) (2013) 1245–1255.
[52] A. Louvi, S.G. Tsitilou, A cDNA clone encoding the ADP/ATP translocase of *Drosophila melanogaster* shows a high degree of similarity with the mammalian ADP/ATP translocases, J. Mol. Evol. 35 (1) (1992) 44–50.
[53] A. Vozza, F. De Leonardis, E. Paradies, A. De Grassi, C.L. Pierri, G. Parisi, C. M. Marobbio, F.M. Lasorsa, L. Muto, L. Capobianco, V. Dolce, S. Raho, G. Fiermonte, Biochemical characterization of a new mitochondrial transporter of dephosphocoenzyme A in *Drosophila melanogaster*, Biochim. Biophys. Acta 1858 (2) (2017) 137–146.
[54] J.P. Venables, J. Tazi, F. Juge, Regulated functional alternative splicing in Drosophila, Nucleic Acids Res. 40 (1) (2012) 1–10.
[55] V. Zara, V. Dolce, L. Capobianco, A. Ferramosca, P. Papatheodorou, J. Rassow, F. Palmieri, Biogenesis of eel liver citrate carrier (CIC): negative charges can substitute for positive charges in the presequence, J. Mol. Biol. 365 (4) (2007) 958–967.
[56] G. Moreno-Hagelsieb, K. Latimer, Choosing BLAST options for better detection of orthologs as reciprocal best hits, Bioinformatics 24 (3) (2008) 319–324.
[57] C. Burge, S. Karlin, Prediction of complete gene structures in human genomic DNA, J. Mol. Biol. 268 (1) (1997) 78–94.
[58] R. Carrozzo, A. Torraco, G. Fiermonte, D. Martinelli, M. Di Nottia, T. Rizza, A. Vozza, D. Verrigni, D. Diodato, G. Parisi, A. Maiorana, C. Rizzo, C.L. Pierri, S. Zucano, F. Piemonte, E. Bertini, C. Dionisi-Vici, Riboflavin responsive mitochondrial myopathy is a new phenotype of dihydrolipoamide dehydrogenase deficiency. The chaperon-like effect of vitamin B2, Mitochondrion 18 (2014) 49–57.
[59] A.R. Cappello, R. Curcio, R. Lappano, M. Maggiolini, V. Dolce, The Physiopathological role of the exchangers belonging to the SLC37 family, Front. Chem. 6 (2018) 122.
[60] D. Porcelli, P. Barsanti, G. Pesole, C. Caggese, The nuclear OXPHOS genes in insecta: a common evolutionary origin, a common cis-regulatory motif, a common destiny for gene duplicates, BMC Evol. Biol. 7 (2007) 215.
[61] S. Avino, P. De Marco, F. Cirillo, M.F. Santolla, E.M. De Francesco, M.G. Perri, D. Rigiracciolo, V. Dolce, A. Belfiore, M. Maggiolini, R. Lappano, A. Vivacqua, Stimulatory actions of IGF-I are mediated by IGF-IR cross-talk with GPER and DDR1 in mesothelioma and lung cancer cells, Oncotarget 7 (33) (2016) 52710–52728.
[62] V. Bartella, E.M. De Francesco, M.G. Perri, R. Curcio, V. Dolce, M. Maggiolini, A. Vivacqua, The G protein estrogen receptor (GPER) is regulated by endothelin-1 mediated signaling in cancer cells, Cell. Signal. 28 (2) (2016) 61–71.
[63] A. Santoro, A.R. Cappello, M. Madeo, E. Martello, D. Iacopetta, V. Dolce, Interaction of fosfomycin with the glycerol 3-phosphate transporter of Escherichia coli, Biochim. Biophys. Acta 1810 (12) (2011) 1323–1329.
[64] S.N. Ho, H.D. Hunt, R.M. Horton, J.K. Pullen, L.R. Pease, Site-directed mutagenesis by overlap extension using the polymerase chain reaction, Gene 77 (1) (1989) 51–59.
[65] D. Bonofiglio, A. Santoro, E. Martello, D. Vizza, D. Rovito, A.R. Cappello, I. Barone, C. Giordano, S. Panza, S. Catalano, V. Iacobazzi, V. Dolce, S. Ando, Mechanisms of divergent effects of activated peroxisome proliferator-activated receptor-gamma on mitochondrial citrate carrier expression in 3T3-L1 fibroblasts and mature adipocytes, Biochim. Biophys. Acta 1831 (6) (2013) 1027–1036.
[66] A. Napoli, D. Aiello, G. Aiello, M.S. Cappello, L. Di Donna, F. Mazzotti, S. Materazzi, M. Fiorillo, G. Sindona, Mass spectrometry-based proteomic approach in Oenococcus oeni enological starter, J. Proteome Res. 13 (6) (2014) 2856–2866.
[67] R. Curcio, D. Aiello, A. Vozza, L. Muto, E. Martello, A.R. Cappello, L. Capobianco, G. Fiermonte, C. Siciliano, A. Napoli, V. Dolce, Cloning, purification, and characterization of the catalytic C-terminal domain of the human 3-hydroxy-3-methyl glutaryl-CoA reductase: an effective, fast, and easy method for testing hypocholesterolemic compounds, Mol. Biotechnol. 62 (2) (2020) 119–131.
[68] V. Kurauskas, A. Hessel, P. Ma, P. Lunetti, K. Weinhaupl, L. Imbert, B. Brutscher, M. S. King, R. Sounier, V. Dolce, E.R.S. Kunji, L. Capobianco, C. Chipot, F. Dehez, B. Bersch, P. Schanda, How detergent impacts membrane proteins: atomic-level views of mitochondrial carriers in Dodecylphosphocholine, J. Phys. Chem. Lett. 9 (5) (2018) 933–938.
[69] R. Curcio, L. Muto, C.L. Pierri, A. Montalto, G. Lauria, A. Onofrio, M. Fiorillo, G. Fiermonte, P. Lunetti, A. Vozza, L. Capobianco, A.R. Cappello, V. Dolce, New insights about the structural rearrangements required for substrate translocation in the bovine mitochondrial oxoglutarate carrier, Biochim. Biophys. Acta 1864 (11) (2016) 1473–1480.
[70] Y. Li, A.R. Cappello, L. Muto, E. Martello, M. Madeo, R. Curcio, P. Lunetti, S. Raho, F. Zaffino, L. Frattaruolo, R. Lappano, R. Malivindi, M. Maggiolini, D. Aiello, C. Piazzolla, L. Capobianco, G. Fiermonte, V. Dolce, Functional characterization of the partially purified Sac1p independent adenine nucleotide transport system (ANTS) from yeast endoplasmic reticulum, J. Biochem. 164 (4) (2018) 313–322.
[71] F. Palmieri, M. Klingenberg, Direct methods for measuring metabolite transport and distribution in mitochondria, Methods Enzymol. 56 (1979) 279–301.
[72] L. Contreras, P. Gomez-Puertas, M. Iijima, K. Kobayashi, T. Saheki, J. Satrustegui, Ca2+ activation kinetics of the two aspartate-glutamate mitochondrial carriers, aralar and citrin: role in the heart malate-aspartate NADH shuttle, J. Biol. Chem. 282 (10) (2007) 7098–7106.
[73] S. Raho, L. Capobianco, R. Malivindi, A. Vozza, C. Piazzolla, F. De Leonardis, R. Gorgoglione, P. Scarcia, F. Pezzuto, G. Agrimi, S.N. Barile, I. Pisano, S. J. Reshkin, M.R. Greco, R.A. Cardone, V. Rago, Y. Li, C.M.T. Marobbio, W. Sommergruber, C.L. Riley, F.M. Lasorsa, E. Mills, M.C. Vegliante, G.E. De Benedetto, D. Fratantonio, L. Palmieri, V. Dolce, G. Fiermonte, KRAS-regulated glutamine metabolism requires UCP2-mediated aspartate transport to support pancreatic cancer growth, Nat. Metab. 2 (12) (2020) 1373–1381.

[74] H. Ito, Y. Fukuda, K. Murata, A. Kimura, Transformation of intact yeast cells treated with alkali cations, J. Bacteriol. 153 (1) (1983) 163–168.
[75] L. Frattaruolo, M. Fiorillo, M. Brindisi, R. Curcio, V. Dolce, R. Lacret, A.W. Truman, F. Sotgia, M.P. Lisanti, A.R. Cappello, Thioalbamide, a thioamidated peptide from amycolatopsis alba, affects tumor growth and stemness by inducing metabolic dysfunction and oxidative stress, Cells 8 (11) (2019).
[76] M. Madeo, C. Carrisi, D. Iacopetta, L. Capobianco, A.R. Cappello, C. Bucci, F. Palmieri, G. Mazzeo, A. Montalto, V. Dolce, Abundant expression and purification of biologically active mitochondrial citrate carrier in baculovirus-infected insect cells, J. Bioenerg. Biomembr. 41 (3) (2009) 289–297.
[77] J. Dandurand, A. Ostuni, M.F. Armentano, M.A. Crudele, V. Dolce, F. Marra, V. Samouillan, F. Bisaccia, Calorimetry and FTIR reveal the ability of URG7 protein to modify the aggregation state of both cell lysate and amylogenic α-synuclein, AIMS Biophys. 7 (3) (2020) 189–203.
[78] O.I. Parisi, M. Fiorillo, L. Scrivano, M.S. Sinicropi, V. Dolce, D. Iacopetta, F. Puoci, A.R. Cappello, Sericin/poly(ethylcyanoacrylate) nanospheres by interfacial polymerization for enhanced bioefficacy of fenofibrate: in vitro and in vivo studies, Biomacromolecules 16 (10) (2015) 3126–3133.
[79] M. Fiorillo, M. Peiris-Pages, R. Sanchez-Alvarez, L. Bartella, L. Di Donna, V. Dolce, G. Sindona, F. Sotgia, A.R. Cappello, M.P. Lisanti, Bergamot natural products eradicate cancer stem cells (CSCs) by targeting mevalonate, Rho-GDI-signalling and mitochondrial metabolism, Biochim. Biophys. Acta 1859 (9) (2018) 984–996.
[80] C. Carrisi, A. Romano, P. Lunetti, D. Antonucci, T. Verri, G.E. De Benedetto, V. Dolce, F.P. Fanizzi, M. Benedetti, L. Capobianco, Platinated nucleotides are substrates for the human mitochondrial deoxynucleotide carrier (DNC) and DNA polymerase γ: relevance for the development of new platinum-based drugs, ChemistrySelect 1 (15) (2016) 4633–4637.
[81] V. Dolce, A.R. Cappello, L. Capobianco, Mitochondrial tricarboxylate and dicarboxylate-Tricarboxylate carriers: from animals to plants, IUBMB Life 66 (7) (2014) 462–471.
[82] M. Santoro, C. Guido, F. De Amicis, D. Sisci, E. Cione, V. Dolce, A. Dona, M. L. Panno, S. Aquila, Bergapten induces metabolic reprogramming in breast cancer cells, Oncol. Rep. 35 (1) (2016) 568–576.
[83] M. Bonesi, M. Brindisi, B. Armentano, R. Curcio, V. Sicari, M.R. Loizzo, M. S. Cappello, G. Bedini, L. Peruzzi, R. Tundis, Exploring the anti-proliferative, pro-apoptotic, and antioxidant properties of Santolina corsica Jord. & Fourr. (Asteraceae), Biomed. Pharmacother. 107 (2018) 967–978.
[84] D. Vergara, M. Bianco, R. Pagano, P. Priore, P. Lunetti, F. Guerra, S. Bettini, S. Carallo, A. Zizzari, E. Pitotti, L. Giotta, L. Capobianco, C. Bucci, L. Valli, M. Maffia, V. Arima, A. Gaballo, An SPR based immunoassay for the sensitive detection of the soluble epithelial marker E-cadherin, Nanomedicine 14 (7) (2018) 1963–1971.
[85] A. del Arco, J. Satrustegui, Molecular cloning of Aralar, a new member of the mitochondrial carrier superfamily that binds calcium and is present in human muscle and brain, J. Biol. Chem. 273 (36) (1998) 23327–23334.
[86] I. Jungreis, C.S. Chan, R.M. Waterhouse, G. Fields, M.F. Lin, M. Kellis, Evolutionary dynamics of abundant stop codon readthrough, Mol. Biol. Evol. 33 (12) (2016) 3108–3132.
[87] M. Sardiello, G. Tripoli, A. Romito, C. Minervini, L. Viggiano, C. Caggese, G. Pesole, Energy biogenesis: one key for coordinating two genomes, Trends Genet. 21 (1) (2005) 12–16.
[88] P. Rehm, J. Borner, K. Meusemann, B.M. von Reumont, S. Simon, H. Hadrys, B. Misof, T. Burmester, Dating the arthropod tree based on large-scale transcriptome data, Mol. Phylogenet. Evol. 61 (3) (2011) 880–887.
[89] J.B. Brown, N. Boley, R. Eisman, G.E. May, M.H. Stoiber, M.O. Duff, B.W. Booth, J. Wen, S. Park, A.M. Suzuki, K.H. Wan, C. Yu, D. Zhang, J.W. Carlson, L. Cherbas, B.D. Eads, D. Miller, K. Mockaitis, J. Roberts, C.A. Davis, E. Frise, A.S. Hammonds, S. Olson, S. Shenker, D. Sturgill, A.A. Samsonova, R. Weiszmann, G. Robinson, J. Hernandez, J. Andrews, P.J. Bickel, P. Carninci, P. Cherbas, T.R. Gingeras, R. A. Hoskins, T.C. Kaufman, E.C. Lai, B. Oliver, N. Perrimon, B.R. Graveley, S. E. Celniker, et al., Nature 512 (7515) (2014) 393–399.
[90] S. Cavero, A. Vozza, A. del Arco, L. Palmieri, A. Villa, E. Blanco, M.J. Runswick, J. E. Walker, S. Cerdan, F. Palmieri, J. Satrustegui, Identification and metabolic role of the mitochondrial aspartate-glutamate transporter in Saccharomyces cerevisiae, Mol. Microbiol. 50 (4) (2003) 1257–1269.
[91] P.N. An, M. Yamaguchi, T. Bamba, E. Fukusaki, Metabolome analysis of *Drosophila melanogaster* during embryogenesis, PLoS One 9 (8) (2014), e99519.
[92] D.K. Hoshizaki, Fat-cell development, in: Complete Molecular Insect Science 2, 2005, pp. 315–345.